

## Polyamine-Vectored Iron Chelators: The Role of Charge

Raymond J. Bergeron,\* Neelam Bharti, Jan Wiegand, James S. McManis, Hua Yao, and Laszlo Prokai

Department of Medicinal Chemistry, University of Florida, Gainesville, Florida 32610-0485

Received December 20, 2004

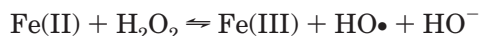
The utility of polyamines as vectors for the intracellular transport of iron chelators is further described. Consistent with earlier results with polyamine analogues, these studies underscore the importance of charge in the design of polyamine-vectored chelators. Four polyamine conjugates are synthesized, two of terephthalic acid [*N*<sup>1</sup>-(4-carboxy)benzoylspermine (**7**) and its methyl ester (**6**)] and two of (*S*)-2-(2,4-dihydroxyphenyl)-4,5-dihydro-4-methyl-4-thiazolecarboxylic acid [(*S*)-4'-(HO)-DADFT] [(*S*)-4,5-dihydro-2-[2-hydroxy-4-(12-amino-5,9-diazadodecyl-oxo)phenyl]-4-methyl-4-thiazolecarboxylic acid (**10**) and its ethyl ester (**9**)]. These four molecules were evaluated in murine leukemia L1210 cells for their impact on cell proliferation (48- and 96-h IC<sub>50</sub> values), their ability to compete with spermidine for the polyamine transport apparatus (*K*<sub>i</sub>), and their intracellular accumulation. The data revealed that when neutral molecules (cargo fragments) were fixed to the polyamine vector, the conjugates competed well with spermidine for transport and were accumulated intracellularly to millimolar levels. However, this was not the case when the cargo fragments were negatively charged. Metabolic studies of the polyamine-vectored (*S*)-4'-(HO)-DADFTs in rodents indicated that not only did the expected deaminopropylation step occur, but also a surprisingly high level of oxidative deamination at the terminal primary nitrogens took place. Finally, the iron-clearing efficiency of the (*S*)-4'-(HO)-DADFT conjugates was determined in a bile-duct-cannulated rodent model. Attaching the ligand to a polyamine vector had a profound effect on increasing the iron-clearing efficiency of this chelator relative to its parent drug.

### Introduction

It has now become clear that manipulation of iron levels in particular biological compartments can have a profound effect on a number of disease processes. The progress of disorders as diverse as Cooley's anemia (also known as  $\beta$ -thalassemia major, a hereditary anemia), Parkinson's disease, and reperfusion injury is known to be iron-dependent.<sup>1–5</sup>

The low solubility of the predominant form of the metal, iron(III) hydroxide (*K*<sub>sp</sub> = 1 × 10<sup>-39</sup>),<sup>6</sup> in the biosphere has necessitated the development of rather sophisticated iron storage and transport systems in nature. Microorganisms utilize low molecular weight ligands, siderophores; higher eukaryotes tend to employ proteins to transport iron (e.g., transferrin) and store iron (e.g., ferritin).<sup>7–9</sup> However, although the metal is critical to life processes, it can be problematic if not properly managed.

The deleterious effects of excess iron are derived from its interaction with reactive oxygen species, such as endogenous hydrogen peroxide (H<sub>2</sub>O<sub>2</sub>). Hydrogen peroxide can, in the presence of Fe(II), be reduced to the hydroxyl radical (HO•) and HO<sup>-</sup> with concomitant oxidation of Fe(II) to Fe(III), the Fenton reaction:



The hydroxyl radical is a powerful oxidizing agent, reacting at a diffusion-controlled rate with many different biomolecules. These processes further initiate

radical chain reactions, causing significant damage to cell constituents, resulting in cell death.<sup>10–12</sup> Because there are any number of physiological reductants, such as O<sub>2</sub><sup>-</sup> and ascorbate, that can reduce Fe(III) back to Fe(II), the Fenton reaction is a cyclical process.

In primates, iron metabolism is highly efficient.<sup>13–17</sup> Little of the metal is absorbed, and no specific mechanism exists for its elimination. Because it cannot be effectively cleared, the introduction of excess iron into this closed metabolic loop leads to chronic overload and ultimately to peroxidative tissue damage.<sup>18–20</sup> For example, patients with severe hemolytic anemias such as  $\beta$ -thalassemia require continued transfusions, which increase their body iron load by 200–250 mg/unit of blood. Unless these individuals receive chelation therapy, they frequently die in their third decade from complications associated with iron overload. Because the liver can no longer manage the iron through the ferritin storage pool, the metal becomes available for Fenton chemistry. Whereas such transfusional iron overload disorders are often presumed to be global in nature, the principal target organs are the liver,<sup>21–23</sup> pancreas,<sup>24,25</sup> and, most critically, the heart.<sup>26–28</sup> The solution is simple: To access, sequester, and promote the excretion of unmanaged iron.

The iron-chelating agents now in use or under clinical evaluation are desferrioxamine B (DFO, Desferal), 1,2-dimethyl-3-hydroxypyridin-4-one (Deferiprone, L1), 4-[3,5-bis(2-hydroxyphenyl)-1,2,4-triazol-1-yl]benzoic acid (ICL670A), and our own desferrithiocin (DFT) analogue, (*S*)-4'-(HO)-DADFT [formal name (*S*)-2-(2,4-dihydroxyphenyl)-4,5-dihydro-4-methyl-4-thiazolecarboxylic acid]. DFO<sup>29</sup> is poorly absorbed from the gastrointestinal (GI)

\* Corresponding author. Phone: (352) 846-1956. Fax: (352) 392-8406. E-mail: bergeron@mc.cop.ufl.edu.

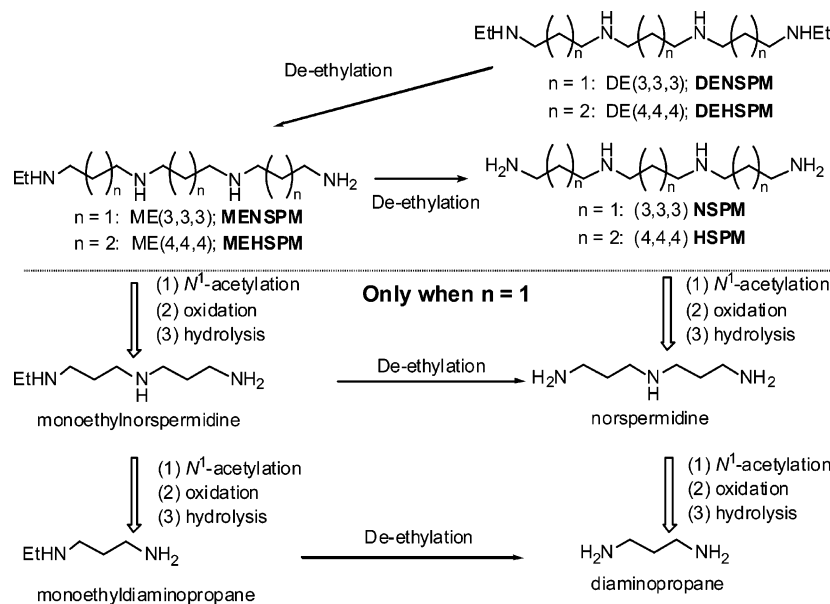


**Figure 1.** Metabolism of diethylnorspermine [DENSPM; DE(3,3,3)] and diethylhomospermine [DEHSPM; DE(4,4,4)]. For clarity, the metabolic byproducts are not shown.

tract and rapidly eliminated from the circulation, necessitating prolonged (8–12 h daily) parenteral [subcutaneous (sc) or intravenous (iv)] infusion.<sup>30–33</sup> Patients have compliance issues, and considerable effort has been devoted to finding suitable alternatives. L1, an orally active bidentate hydroxypyridinone, does not clear iron well.<sup>1,34–37</sup> ICL670A has a very narrow therapeutic window, owing to potential nephrotoxicity. There are also concerns about genotoxicity and reproductive physiology.<sup>38–40</sup>

Desferrithiocin (DFT), a natural product iron chelator (siderophore) isolated from *Streptomyces antibioticus*, is one of the most orally effective deferrating agents yet identified, but renal toxicity precluded its clinical use. Our subsequent systematic structure–activity studies have afforded the orally active DFT analogue (*S*)-4′-(HO)-DADFT, now in phase I/II clinical trials in patients with iron overload. We were also able to further tailor the (*S*)-desazadesmethyldeferrithiocin [formal name (*S*)-4,5-dihydro-2-(2-hydroxyphenyl)-4-thiazolecarboxylic acid] platform both to increase iron-clearing efficiency and to target specific organs. Ligands were assembled that achieved high levels in the organs most affected in iron overload diseases, i.e., liver, pancreas, and heart. The magnitude of the structure–activity investigation required to achieve this goal was not insignificant.<sup>41–47</sup> This work coupled with previous DFT structure–activity exploration underscores the need for a more universal tool for delivering iron chelators intracellularly, not just desferrithiocin analogues, but chelators in general. Thus, the current paper further explores the utility of polyamines as vectors for enhanced intracellular delivery of iron chelators.

## Results and Discussion

**Design Considerations.** The current investigation addresses three issues: (1) the significance of charge in exploiting the polyamine transport machinery as a conduit for intracellular transport of polyamine-linked chelators,<sup>48</sup> (2) the metabolic profile of the polyamine-vectored iron chelators,<sup>49–51</sup> and (3) the impact of the

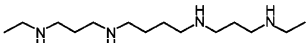
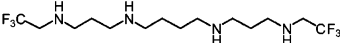
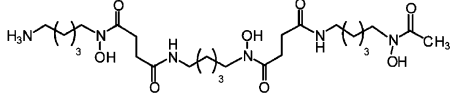
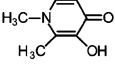
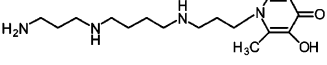
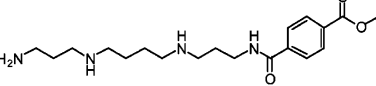
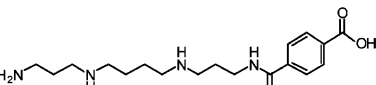
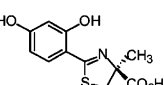
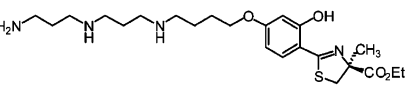
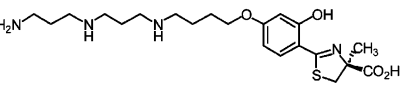
vectoring on the iron-clearing efficiency of (*S*)-4′-(HO)-DADFT in rodents.<sup>41,45,52</sup>

Polyamines [e.g. putrescine (PUT), spermidine (SPD), and spermine (SPM)], like iron, are requisite entities for the function of nearly all eukaryotes and prokaryotes. These molecules, which are polycationic at physiological pH, are necessary for a number of cellular processes.<sup>53</sup> In eukaryotes, PUT, SPD, and SPM are the most common polyamines. Their biosynthesis begins with the conversion of ornithine to PUT via the enzyme ornithine decarboxylase (ODC), followed by aminopropylation to SPD using decarboxylated *S*-adenosylmethionine via spermidine synthase.<sup>54</sup> A second aminopropylation of SPD occurs via spermine synthase to afford SPM. Almost all animal cells also have a transport apparatus for importing these molecules that is capable of concentrating them against a gradient to millimolar levels.<sup>54–56</sup> Catabolically, SPM is acetylated to  $N^1$ -acetylspermine by spermidine-spermine  $N^1$ -acetyltransferase (SSAT); this is oxidized to 3-acetamidopropanal and SPD via polyamine oxidase (PAO). Spermidine is then  $N^1$ -acetylated, oxidized, and hydrolyzed to PUT and a second mole of 3-acetamidopropanal.<sup>54</sup> It is important to note that this acetylation and oxidation occur at the primary amine on the 3-aminopropyl fragment, not the 4-aminobutyl end of the molecule.

For example, as shown in Figure 1, in the liver,  $N^1,N^{11}$ -diethylnorspermine [DENSPM; DE(3,3,3)] is deethylated once to generate monoethylnorspermine and a second time to afford norspermine; the 3-aminopropyl fragments are then cleaved from both of these products. However, aminobutyl fragments cannot be processed; catabolism of  $N^1,N^{14}$ -diethylhomospermine [DEHSPM; DE(4,4,4)] cannot proceed past de-ethylation.<sup>49–51</sup> Thus, when a polyamine vector is attached to a ligand, the metabolism of the polyamine moiety would be expected to terminate at an aminobutyl segment.

In previous studies, we have mapped the structural boundary conditions set by the polyamine transport apparatus on polyamine analogues.<sup>48,57–68</sup> Although steric issues are important,<sup>48,58,65,66</sup> charge is critical to

**Table 1.** L1210 Cell Growth Inhibition and Transport for Selected Polyamines, Iron Chelators, and Polyamine Conjugate Iron Chelators

compound structure/abbreviation	IC <sub>50</sub> (μM) <sup>a</sup>		K <sub>i</sub> (μM) <sup>b</sup>	intracellular conc/ treatment conc.	
	48 h	96 h		intracellular conc <sup>c</sup>	treatment conc.
 DESPM (1) <sup>d</sup>	30	0.2	1.6	400 (treatment conc. 30 μM)	13.3
 FDESPM (2) <sup>e</sup>	–	> 100	285	< 20 (treatment conc. 100 μM)	< 0.2
 DFO (3)	7	6	>500	Not detectable	–
 L1 (4) <sup>f</sup>	46	55	>500	~1 (treatment conc. 50 μM)	0.02
 L1-SPM-conjugate (5) <sup>f</sup>	0.2	0.2	3.7	390 (treatment conc. 0.2 μM)	1950
 NTS-ME (6)	> 100	> 100	3.1	430 (treatment conc. 100 μM for 48 h)	4.3
 NTS (7)	> 100	> 100	27	< 70 (treatment conc. 100 μM)	< 0.7
 (S)-4'-(HO)-DADFT (8)	19	20	> 500	< 50 (treatment conc. 100 μM)	< 0.5
 NSPD-(S)-4'-(HO)-DADFT-EE (9)	1.5	1.5	5.7	947 (9); 2980 (10) (treatment conc. 100 μM for 4 h)	9.5 (9) 29.8 (10)
 NSPD-(S)-4'-(HO)-DADFT (10)	40	40	73	71 (treatment conc. 100 μM for 4 h)	0.7

<sup>a</sup> The IC<sub>50</sub> was estimated from growth curves for L1210 cells grown in the presence of nine different extracellular concentrations of drug spanning four logarithmic units: 0, 0.03, 0.1, 0.3, 1.0, 3, 10, 30, and 100 μM. IC<sub>50</sub> data are presented as the mean of at least two experiments with variation from the mean typically 10–25% for the 96-h IC<sub>50</sub> values. <sup>b</sup> K<sub>i</sub> determinations were made by following analogue inhibition of spermidine transport. All polyamine analogues exhibited simple substrate-competitive inhibition of [<sup>3</sup>H]SPD transport by L1210 cells. Values reported in the table represent the mean of at least two or three experiments with a variation typically less than 10%. <sup>c</sup> Unless otherwise indicated, the cells were treated for 48 h. Intracellular concentration is expressed as pmol/10<sup>6</sup> cells. Untreated L1210 cells (10<sup>6</sup>) correspond to about 1 μL volume; therefore, the concentration can be estimated as micromolar. The reported values represent the mean of triplicate determinations. <sup>d</sup> Reproduced from ref 65. <sup>e</sup> Reproduced from ref 48. <sup>f</sup> Reproduced from ref 72.

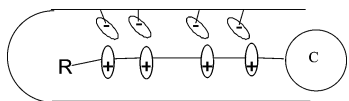


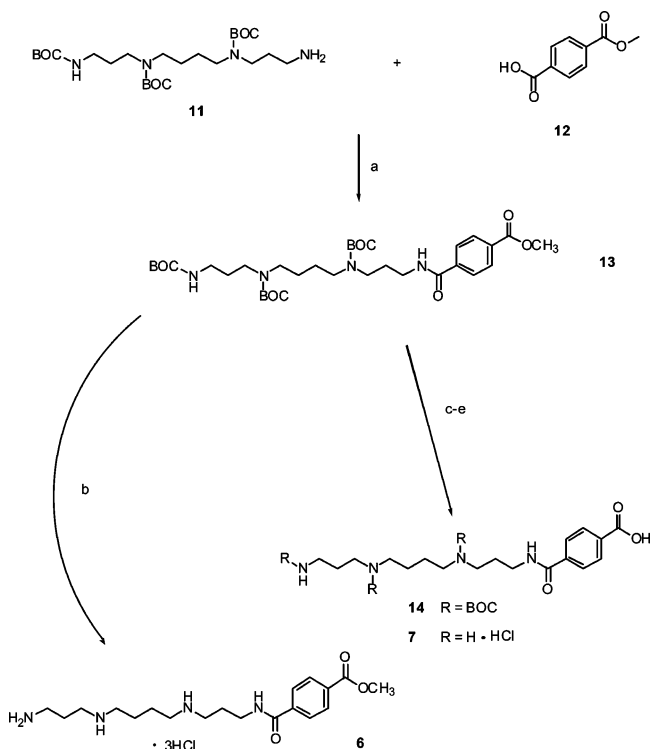
**Figure 2.** A schematic representation of the polyamine transport apparatus complex; R = H, alkyl; C = chelator or other cargo to be vectored. In principle, C could be neutral or positively or negatively charged.

recognition and transport of these substrates (Table 1).<sup>48,58,65,68–70</sup> For example, *N*<sup>1</sup>,*N*<sup>12</sup>-diethylspermine (DESPM, **1**, Table 1), a tetracation at physiological pH, competes well with spermidine for the polyamine transport apparatus and is concentrated to millimolar levels intracellularly. The DESPM analogue *N*<sup>1</sup>,*N*<sup>12</sup>-bis(2,2,2-trifluoroethyl)spermine (FDESPM, **2**) is dicationic at pH 7.4 and competes poorly with spermidine for the polyamine transport apparatus. In the picture that emerges (Figure 2), the polyamine transport apparatus provides biological counteranions for the cationic nitrogens. On the basis of simple electrostatics, it would seem that when a polyamine is used to vector a cargo molecule C intracellularly, the charge of C is critical. When C is neutral or positively charged, binding to the transporter should be more favorable; when C is negatively charged, it should be weak.<sup>48,58,65,66,71</sup>

In an earlier study, we assessed the feasibility of vectoring iron chelators intracellularly via the polyamine transporter.<sup>72</sup> A simple bidentate, neutral ligand, L1 (**4**, Table 1), was conjugated to SPM in two steps, generating 1-(12-amino-4,9-diazadodecyl)-2-methyl-3-hydroxy-4(1*H*)-pyridinone (**5**). Job's plots revealed that **5** forms the expected 3:1 ligand/Fe(III) complex; furthermore, the chelator fragment C is neutral. All parameters measured in murine leukemia L1210 cells treated with this conjugate, including (1) the effect on cell proliferation (IC<sub>50</sub> values), (2) the ability to compete with radiolabeled spermidine for the polyamine transport apparatus (*K*<sub>i</sub>), (3) impact on polyamine pools, and (4) effects on the polyamine enzymes ODC, *S*-adenosylmethionine decarboxylase (AdoMetDC), and SSAT, suggested that this ligand conjugate both competed well for the polyamine transport apparatus and indeed gained intracellular access (390 μM). L1 (**4**) itself does not achieve high intracellular concentrations (~1 μM) in cultured cells.

The ligand donors in iron chelators are generally highly polar and/or often ionizable, e.g., carboxylates. Thus, while neutral chelator polyamine conjugates, i.e., the L1 conjugate, are transported intracellularly, those in which the cargo fragment is negatively charged at physiological pH (i.e., carboxylates) are not likely to be taken up by cells. To substantiate this concern and establish how to circumvent the negative charge problem, two kinds of polyamine conjugates were evaluated: those with a free carboxyl and the corresponding alkyl esters. The cargo molecules (Table 1) include terephthalic acid and its monomethyl ester, and (*S*)-4'-(HO)-DADFT (**8**) and its ethyl ester. The terephthalic acid fragments were affixed to SPM via an amide linkage (**6** and **7**); the (*S*)-4'-(HO)-DADFT moieties were attached to norspermidine (NSPD) at the C-4'-oxygen through a butyl group (**9** and **10**). While all of these vectored compounds still have three protonated positively charged nitrogens at physiological pH, the terephthalic acid and (*S*)-4'-(HO)-DADFT acid conjugates

### Scheme 1. Synthesis of SPD-terephthalates **6** and **7**<sup>a</sup>



<sup>a</sup> Reagents: (a) CDI, CH<sub>2</sub>Cl<sub>2</sub>, 77%; (b) HCl, CH<sub>3</sub>OH, 84%; (c) 1 N NaOH, CH<sub>3</sub>OH, then 1 N HCl; (d) TFA, CH<sub>2</sub>Cl<sub>2</sub>; (e) ion exchange, 58%.

(**7** and **10**) each present a negatively charged cargo fragment, C, the carboxylate, to the transport apparatus. The cargo fragment of their corresponding esters (**6** and **9**) is neutral.

**Synthesis of Terephthalic Acid Conjugates (**6** and **7**).** The terephthalic acid conjugate was chosen as the first model because (1) the size and sweep volume for this fragment are similar to those of L1 in the SPM–L1 conjugate (**5**, Table 1), which utilizes the polyamine transport machinery for intracellular access; (2) the compatibility of an amide linkage with the vectoring concept needed clarification; and (3) the conjugate cargo could be rendered neutral, as in the methyl ester (**6**), or negatively charged, as in the acid (**7**). Terminally monoacylated spermine **7** and its methyl ester **6** were accessed according to Scheme 1. *N*<sup>1</sup>,*N*<sup>4</sup>,*N*<sup>9</sup>-Tris(*tert*-butoxycarbonyl)spermine (**11**)<sup>73</sup> was acylated in 77% yield with monomethyl terephthalate (**12**), which had been activated with 1,1'-carbonyldiimidazole (CDI). The amine protecting groups of the resulting adduct **13** were removed using methanolic HCl, generating triamino amide methyl ester **6** in 84% yield. Alternatively, initial cleavage of the ester in intermediate **13** with NaOH in aqueous methanol resulted in tris(BOC) acid **14**. The carbamates of **14** were cleaved with trifluoroacetic acid, followed by ion exchange chromatography, providing the terephthalic acid derivative of spermine as its trihydrochloride salt, **7**, in 58% yield from **13**.

**Synthesis of (*S*)-2-(2,4-Dihydroxyphenyl)-4,5-dihydro-4-methyl-4-thiazolecarboxylic Acid [(*S*)-4'-(HO)-DADFT] Polyamine Conjugates and Their Corresponding Metabolic Products.** In addition to the fact that the conjugate cargo could be rendered neutral, these conjugates (**9** and **10**) were chosen to

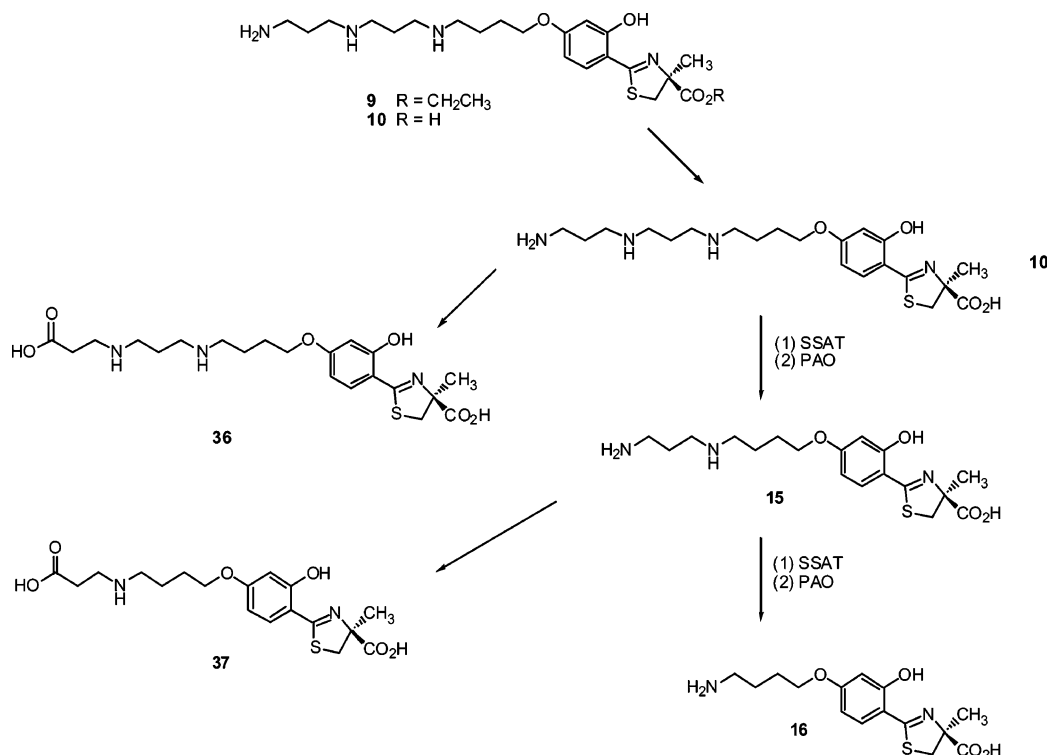


**Figure 3.** Metabolism of the polyamine moiety of the NSPD-(S)-4'-(HO)-DADFT conjugates. The terminal aminopropyl fragments are acetylated by SSAT and oxidized by PAO to afford the diamine (**15**) and, subsequently, the monoamine (**16**).

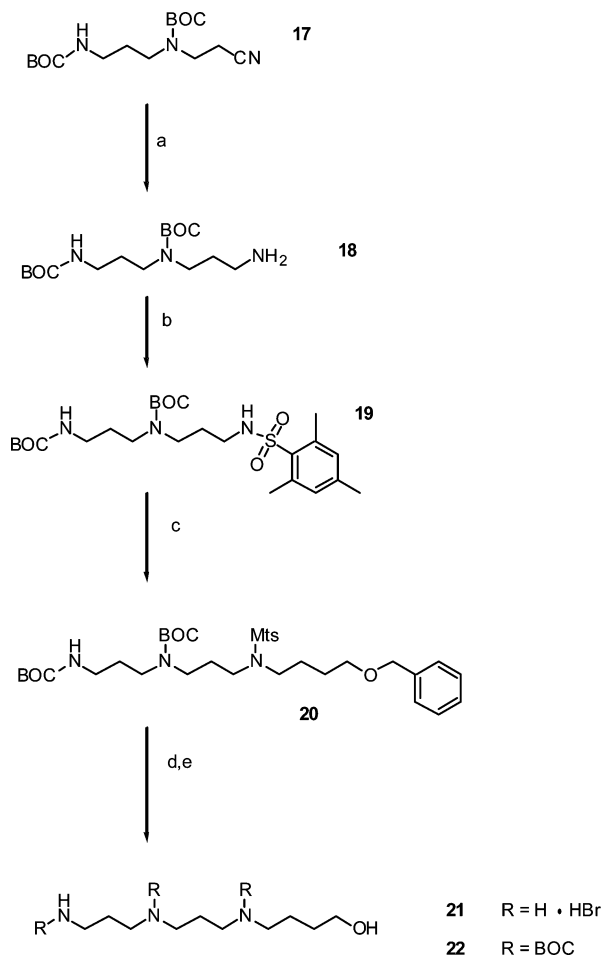
assess the utility of the polyamine vector for iron chelators and to help further circumscribe the structural boundary conditions set by the polyamine transport apparatus on substrate binding and import. The cargo ligand, (S)-4'-(HO)-DADFT (**8**), has already been thoroughly investigated as a therapeutic iron chelator in a variety of animal models.<sup>41,45,52</sup> This chelator, although negatively charged at physiological pH, can be rendered neutral by esterification. In addition, the NSPD backbone, owing to the aminopropyl fragments, should be metabolically labile, providing putative metabolites **15** and **16** (Figure 3).

The key step in the synthesis of norspermidine-(S)-4'-(HO)-DADFT conjugate **10** and its ethyl ester **9** was alkylation of the ethyl ester of (S)-4'-(HO)-DADFT (**24**) at its 4'-hydroxyl with tosylate **23** (Scheme 3). Efficient preparation of the protected triamine with the 4-hydroxybutyl connector at N<sup>1</sup> (**22**) was carried out as in Scheme 2. Bis(BOC)aminonitrile **17**<sup>74,75</sup> was hydrogenated over Raney nickel under highly alkaline conditions<sup>76</sup> to N<sup>1</sup>,N<sup>4</sup>-bis(*tert*-butoxycarbonyl)norspermidine (**18**).<sup>77,78</sup> The  $\omega$ -hydroxy tether was affixed to the amine of **18** in two steps. A mesitylenesulfonyl group<sup>65</sup> was attached to **18** (85% yield for two steps), and the resulting sulfonamide **19** was alkylated with benzyl 4-bromobutyl ether (NaH, DMF), giving benzyl ether **20** in 78% yield. The three nitrogens and the oxygen of **20** were unmasked, employing 30% HBr in HOAc and phenol in CH<sub>2</sub>Cl<sub>2</sub>,<sup>65</sup> and the amino groups of trihydrobromide salt **21** were trapped (BOC<sub>2</sub>O, THF, NEt<sub>3</sub>) as their *tert*-butyl carbamates, furnishing N<sup>1</sup>-(4-hydroxybutyl)-N<sup>4</sup>,N<sup>7</sup>,N<sup>7</sup>-tris(*tert*-butoxycarbonyl)norspermidine (**22**) in 59% yield from **20**.

The alcohol group of norspermidine reagent **22** was activated in 92% yield as tosylate **23** (TsCl, TEA, CH<sub>2</sub>Cl<sub>2</sub>) (Scheme 3). (S)-4'-(HO)-DADFT (**8**) was con-

verted to ethyl (S)-2-(2,4-dihydroxyphenyl)-4,5-dihydro-4-methyl-4-thiazolecarboxylate (**24**) in 96% yield using iodoethane and *N,N*-diisopropylethylamine (DIEA) in DMF. Deprotonation of **24** using NaOEt and heating with tosylate **23** in EtOH effected monoalkylation of the resorcinol system in 67% yield. Structural assignment of **25** was based on selective 4-*O*-alkylation of 2,4-dihydroxybenzoic acid systems<sup>79–82</sup> and on NOESY of final product **10**. Irradiation at 4.18, corresponding to the methylene of the ether function (g), significantly enhanced the aromatic signals at 6.59 (h) and 6.69 (i), as well as an internal methylene of the tetramethylene chain (b) (Figure 4). Similarly, NOE correlations from the methyl group of 2-hydroxy-4-methoxybenzaldehyde (**27**) to the adjacent protons on the aromatic ring (H-3 and H-5) were observed. However, only one ring proton (H-3) was so affected in the analogous experiment with 4-hydroxy-2-methoxybenzaldehyde (**28**). Thus, the 4'-disposition of the *O*-alkyl group of **25** in Scheme 3 was confirmed. Treatment of **25** with ethanolic HCl, generated in situ from acetyl chloride,<sup>83</sup> removed the BOC groups, affording the ethyl ester of the NSPD-(S)-4'-(HO)-DADFT conjugate (**9**) (65%). Saponification of the ester in **25** with NaOH in aqueous methanol resulted in tris(BOC) acid **26** in 63% yield. The carbamates of **26** were cleaved with trifluoroacetic acid (TFA), followed by ion exchange chromatography, providing (S)-4,5-dihydro-2-[2-hydroxy-4-(12-amino-5,9-diazadodecyloxy)phenyl]-4-methyl-4-thiazolecarboxylic acid trihydrochloride (**10**) in 85% yield.

(S)-4,5-Dihydro-2-[2-hydroxy-4-(8-amino-5-azaoctyloxy)phenyl]-4-methyl-4-thiazolecarboxylic acid (**15**), a putative metabolite of the norspermidine-(S)-4'-(HO)-DADFT conjugate **10**, was made by the method of Scheme 4. *N,N'*-Bis(*tert*-butoxycarbonyl)-*N*-(4-hydroxybutyl)-1,3-diaminopropane (**29**)<sup>84</sup> was transformed into

**Scheme 2.** Generation of BOC-Protected NSPD Reagent **20**

<sup>a</sup> Reagents: (a) H<sub>2</sub>, Raney Ni, NaOH, EtOH; (b) mesitylene-sulfonyl chloride, NaOH (aq), CH<sub>2</sub>Cl<sub>2</sub>, 85%; (c) benzyl 4-bromobutyl ether (1.1 equiv), NaH, DMF, 78%; (d) 30% HBr in HOAc, PhOH, CH<sub>2</sub>Cl<sub>2</sub>; (e) BOC<sub>2</sub>O, THF, NEt<sub>3</sub>, 59%.

its tosylate **30** (80%). Resorcinol analogue **24** was treated with **30** and sodium ethoxide (1 equiv) in hot EtOH, resulting in 4'-O-alkylated product **31** in 37% yield. Basic hydrolysis of ester **31** followed by acidification with dilute HCl gave bis(BOC) acid **32** in 77% yield. The amine protecting groups of **32** were cleaved quantitatively with TFA, providing bis(TFA) salt **15**, which would arise from the de-3-aminopropylation of **10**.

(*S*)-4,5-Dihydro-2-[2-hydroxy-4-(4-aminobutoxy)-phenyl]-4-methyl-4-thiazolecarboxylic acid (**16**), the result of successive de-3-aminopropylation of **10**, was synthesized as in Scheme 5. Diphenol **24** was selectively alkylated with the *O*-tosylate of *N*-(*tert*-butoxycarbonyl)-4-amino-1-butanol (**33**),<sup>85</sup> generating alkyl aryl ether **34** in 55% yield. Hydrolysis of ester **34** under alkaline conditions gave BOC acid **35** (63%). The amino group of **35** was deprotected with TFA, affording proposed metabolite **16** in 63% yield.

**Stoichiometry of the Iron(III) Complex of 10.** The stoichiometry of the ferric complexes of **10** was determined spectrophotometrically at  $\lambda_{\text{max}}$  480 nm. The Job's plot of the acid (Figure 5) was in keeping with a 2:1 ligand/metal complex for this analogue, the same as for the nonconjugated counterpart.

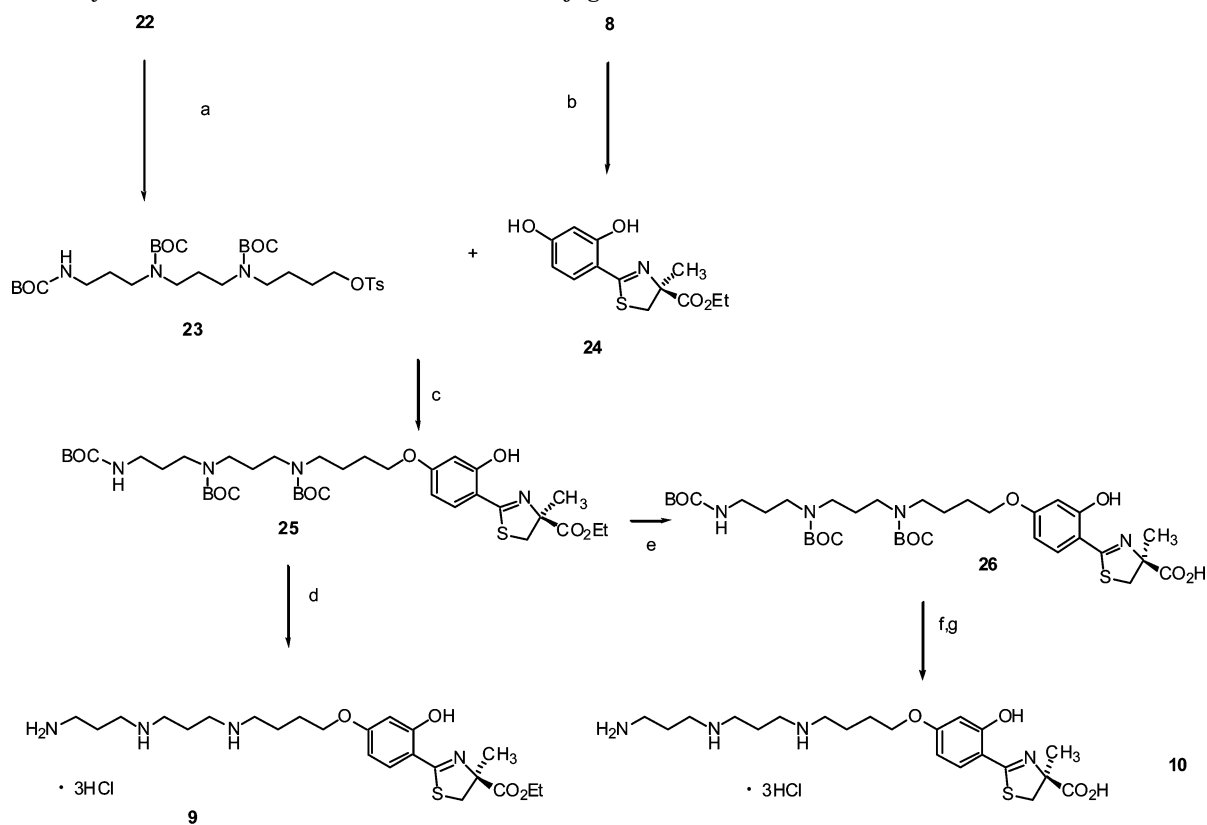
**Polyamine Vectors: Charge Restrictions on Cargo Fragments.** The purpose of this study is to

further define the charge restrictions set by the polyamine transport apparatus on cargo fragments fixed to a polyamine vector. The study answers two different but related questions: (1) How does charge impact on binding of a polyamine cargo conjugate to the polyamine transport apparatus, and (2) how does charge impact on the actual incorporation of polyamine adducts?

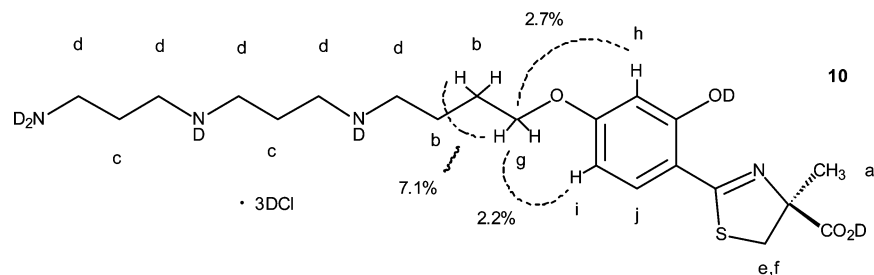
The first measurement addresses the issue of polyamine conjugates that carry a negative charge and how they compete with spermidine for the polyamine transport apparatus. The  $K_i$  values were determined versus [<sup>3</sup>H]SPD. The historic  $K_i$  values for DESPM (**1**),<sup>65</sup> FDESPM (**2**),<sup>48</sup> L1 (**4**),<sup>72</sup> and the L1-polyamine conjugate (**5**)<sup>72</sup> are included for comparative reasons (Table 1). The  $K_i$  for DESPM, a tetracation at physiological pH,<sup>48</sup> is 1.6  $\mu\text{M}$ .<sup>65</sup> The  $\beta,\beta,\beta$ -trifluoroethyl analogue (FDESPM, **2**), which is dicationic at physiological pH, competes poorly with SPD for the transporter ( $K_i$ , 285  $\mu\text{M}$ ). Not surprisingly, the bidentate ligand L1 did not compete for the polyamine transport apparatus at all ( $K_i$ , >500  $\mu\text{M}$ ), whereas its SPM conjugate **5** was an effective competitor ( $K_i$ , 3.7  $\mu\text{M}$ ).<sup>72</sup> When the free carboxyl of the monomethyl ester of terephthalic acid is conjugated to SPD, the resulting monoamide **6**, a trication at physiological pH, does compete well for the transport machinery ( $K_i$ , 3.1  $\mu\text{M}$ ). However, when the methyl ester of the amide is cleaved to the carboxylic acid (**7**), an anion at physiological pH, the  $K_i$  increases 9-fold, to 27  $\mu\text{M}$ . This is in keeping with the picture of the polyamine transport apparatus presented in Figure 2, in which the polyamine cationic centers bind to negative counterions in the transporter. Thus, conjugate **7**, bearing a carboxylate anion, would not be expected either to bind well to the transport apparatus or to be appreciably internalized by the cell. This view is further underscored with the NSPD-(*S*)-4'-(HO)-DADFT conjugates **9** and **10**. Once again, the  $K_i$  for the free acid **10**, which exists as the carboxylate anion under the assay conditions, is substantially (12.8-fold) higher than that of the corresponding carboxylate-neutral ethyl ester **9**, 73 vs 5.7  $\mu\text{M}$ . The question now becomes: Are these data in keeping with cellular uptake?

Previous studies in these and other laboratories demonstrated that the polyamine analogues can achieve rather high intracellular concentrations, even against a strong concentration gradient.<sup>48,65,66</sup> For example, DESPM reaches intracellular levels of 400  $\mu\text{M}$  when the extracellular treatment concentration is 30  $\mu\text{M}$  (Table 1).<sup>65</sup> However, the dicationic FDESPM (**2**), which demonstrated a poor  $K_i$  for the polyamine transport apparatus, was not effectively concentrated in the cell. Even at an extracellular treatment concentration of 100  $\mu\text{M}$ , FDESPM achieved a cellular level of <20  $\mu\text{M}$ . These observations were exploited in our earlier study in which the neutral, bidentate L1 (**4**) was vectored intracellularly by linking it to spermine (**5**).<sup>72</sup> Whereas L1 itself only reached intracellular levels of 1  $\mu\text{M}$  at an extracellular treatment concentration of 50  $\mu\text{M}$ , the conjugate **5** attained an intracellular level of 390  $\mu\text{M}$  at an extracellular concentration of 0.2  $\mu\text{M}$  (Table 1).

This was consistent with the idea that the polyamine transport apparatus could be employed to vector neutral polyamine-conjugated iron chelators. However, it is important to recall that, in general, iron chelators are

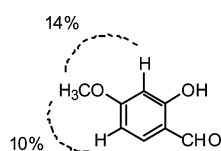
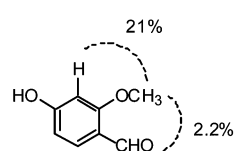
**Scheme 3.** Synthesis of NSPD-(*S*)-4'-(HO)-DADFT Conjugates **9** and **10**

<sup>a</sup> Reagents: (a) TsCl, NEt<sub>3</sub>, CH<sub>2</sub>Cl<sub>2</sub>, 92%; (b) EtI, DIEA, DMF, 96%; (c) Na, CH<sub>3</sub>CH<sub>2</sub>OH, 60 °C, 67%; (d) CH<sub>3</sub>COCl, EtOH, 65%; (e) 1 N NaOH, CH<sub>3</sub>OH, then 1 N HCl, 63%; (f) TFA, CH<sub>2</sub>Cl<sub>2</sub>; (g) ion exchange, 85%.

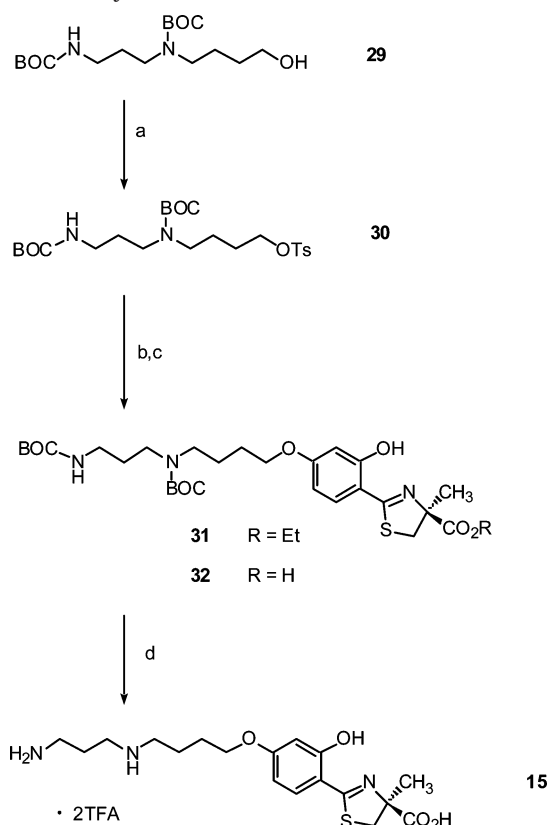


<sup>1</sup>H Assignment (**10**)     $\delta$  (multiplicity, integration, coupling constant in Hz)

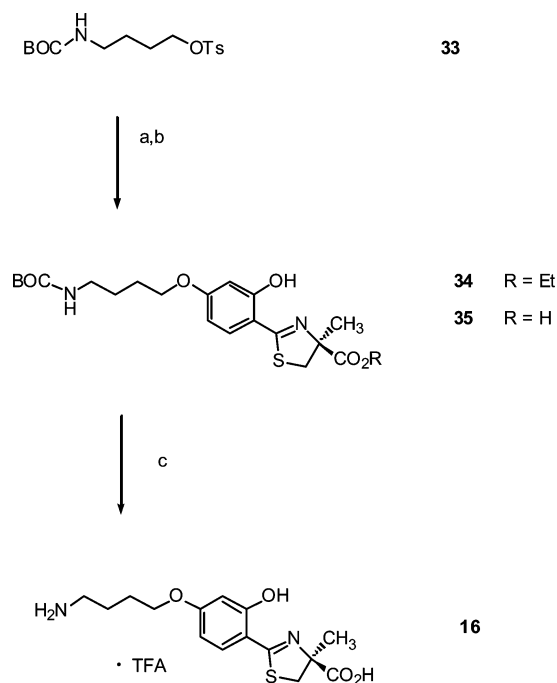
a	1.80 (s, 3 H)
b	1.85-1.92 (m, 4 H)
c	2.07-2.16 (m, 4 H)
d	3.08-3.22 (m, 10 H)
e	3.62 (d, 1 H, <i>J</i> = 11.9)
f	4.00 (d, 1 H, <i>J</i> = 11.9)
g	4.18 (t, 2 H, <i>J</i> = 5.4)
h	6.59 (d, 1 H, <i>J</i> = 2.1)
i	6.69 (dd, 1 H, <i>J</i> = 9.0, 2.1)
j	7.70 (d, 1 H, <i>J</i> = 9.0)

**27****28**

**Figure 4.** <sup>1</sup>H resonances for the (*S*)-4'-(HO)-DADFT conjugate (**10**) and pertinent homonuclear NOESY correlations for **10** and isomeric model systems **27** and **28**. The complete <sup>1</sup>H NMR data for **27** and **28** are in the Supporting Information.

**Scheme 4.** Synthesis of Diamine Metabolite **15**

<sup>a</sup> Reagents: (a) TsCl, NEt<sub>3</sub>, CH<sub>2</sub>Cl<sub>2</sub>, 80%; (b) **24**, Na, CH<sub>3</sub>CH<sub>2</sub>OH, 80 °C, 37%; (c) 1 N NaOH, EtOH, then 1 N HCl, 77%; (d) TFA (quantitative).

**Scheme 5.** Synthesis of Monoamine Metabolite **16**

<sup>a</sup> Reagents: (a) **24**, Na, EtOH, 75 °C, 55%; (b) 1 N NaOH, CH<sub>3</sub>CH<sub>2</sub>OH, then 1 N HCl, 63%; (c) TFA, 63%.

negatively charged at physiological pH, as many of these molecules utilize carboxylate donors. This fact begs the question: How effectively would a polyamine-conjugated, negatively charged ligand be transported intracellularly? The above  $K_i$  studies suggest that

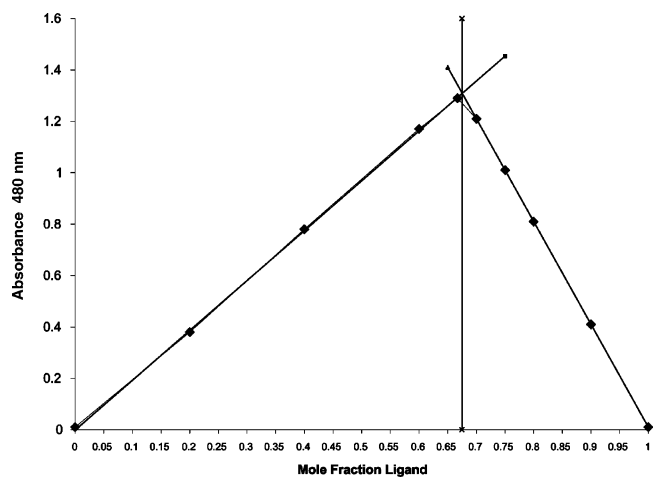


**Figure 5.** Job's plot of **10** ( $\lambda_{\max} = 480$  nm). Solutions containing different ligand/Fe(III) ratios were prepared so that [ligand] + [Fe(III)] = 1.0 mM. The data points were fitted to the mole fractions (1) from 0 to 0.60 and (2) from 0.70 to 1.00;  $r^2 = 0.9997$  (four data points) and 0.9999 (five data points), respectively. The theoretical mole fraction maximum for a 2:1 ligand/Fe complex is 0.667; a linear intercept maximum of 0.675 was found.

negatively charged ligands would be poor candidates for vectoring; this concept was substantiated when intracellular levels of terephthalate conjugates **6** and **7** and NSPD-conjugated desferrithiocin analogues **9** and **10** were compared in L1210 cells.

Cells treated with methyl terephthalate-SPD conjugate **6** at a concentration of 100  $\mu$ M achieved an intracellular drug level of 430  $\mu$ M. However, cells treated with the corresponding acid conjugate (**7**) at a concentration of 100  $\mu$ M did not achieve notable intracellular levels, <70  $\mu$ M.

This same scenario was also observed with the (*S*)-4'-(HO)-DADFT series (**8–10**). In each case, the extracellular treatment concentration was 100  $\mu$ M. Under these treatment conditions, the intracellular concentration of the parent ligand, (*S*)-4'-(HO)-DADFT (**8**), does not exceed 50  $\mu$ M (Table 1). However, the ethyl ester of the NSPD-(*S*)-4'-(HO)-DADFT conjugate (**9**) was effectively transported into the cell, achieving a concentration of  $947 \pm 110$   $\mu$ M; furthermore, the hydrolysis product, acid conjugate **10**, again in cells treated with the ester (**9**) was present at approximately three times the amount of the ester,  $2980 \pm 280$   $\mu$ M. In cells treated with the NSPD conjugate acid **10** itself, the intracellular drug level only rose to about 70  $\mu$ M. In both series (**6/7**, **9/10**), the results are in keeping with the significant drop in  $K_i$  of the esters (**6** and **9**) compared to the corresponding free acid polyamine conjugates (**7** and **10**), substantiating the concept that the transport apparatus rejects substrates that carry a negative charge. Furthermore, it seems likely that the esters **6** and **9** were transported into the cells and then hydrolyzed to the respective free acid.

These results led us to evaluate the behavior of the chelator conjugates vs the parent chelator, i.e., the L1 (**5** vs **4**) and (*S*)-4'-(HO)-DADFT series (**9** and **10** vs **8**), in a rodent iron clearance model.

**Effect of the Conjugates on Cell Proliferation.** It is crucial to understand that although nearly all iron

chelators are effective as growth inhibitors of tumor cells in culture, where the iron sources are limited, this has not been the case in tumor xenografts in whole animals.<sup>86</sup> In the latter instance, there is a continual and ample supply of protein-bound iron, e.g., as transferrin iron. To put this into perspective, the treatment concentration at which cell growth is decreased by 50% relative to untreated controls (IC<sub>50</sub>) of the reference chelator DFO in cultured L1210 murine leukemia cells is under 10  $\mu\text{M}$ , yet the daily recommended dose for patients is 150  $\mu\text{mol/kg}$ .

The IC<sub>50</sub> values were determined at both 48 and 96 h in L1210 cells (Table 1). The values for DESPM (1),<sup>65</sup> FDESPM (2),<sup>48</sup> L1 (4),<sup>72</sup> and the SPM-L1 conjugate (5)<sup>72</sup> are historical but are included in Table 1 for comparative purposes. Although FDESPM (2) is not active in the IC<sub>50</sub> assay (>100  $\mu\text{M}$ ), the behavior of DESPM (1) in the IC<sub>50</sub> assay is typical of many polyamine analogues, that is, the IC<sub>50</sub> decreases as the length of treatment increases, in this case, from 30  $\mu\text{M}$  at 48 h to 0.2  $\mu\text{M}$  at 96 h.

Iron chelators typically maintain a constant IC<sub>50</sub> value as treatment time progresses (Table 1). For example, DFO (3), at the same time points, has IC<sub>50</sub> values of 7  $\mu\text{M}$  (48 h) and 6  $\mu\text{M}$  (96 h); the L1 (4) IC<sub>50</sub> values are somewhat higher, 46 and 55  $\mu\text{M}$  at 48 and 96 h, respectively. Appending a polyamine vector to L1 (5) decreased the IC<sub>50</sub> considerably, to 0.2  $\mu\text{M}$  at both 48 and 96 h.

Consistent with these findings, the IC<sub>50</sub> values for (S)-4'-(HO)-DADFT (8) at 48 and 96 h were within error of each other, 19 and 20  $\mu\text{M}$ , respectively. Although affixing NSPD to the 4'-hydroxyl of (S)-4'-(HO)-DADFT (8) via a butyl linkage to afford NSPD-(S)-4'-(HO)-DADFT (10) increased the 48- and 96-h IC<sub>50</sub> values to 40  $\mu\text{M}$ , conversion of this conjugate to the corresponding ethyl ester (9) decreased the IC<sub>50</sub> to 1.5  $\mu\text{M}$  at both time points. Neither of the terephthalate analogues, *N*<sup>1</sup>-terephthaloylspermine methyl ester (NTS-ME, 6) or *N*<sup>1</sup>-terephthaloylspermine (NTS, 7), had any impact on cell growth; the 48- and 96-h IC<sub>50</sub> values for both compounds were >100  $\mu\text{M}$ .

**Iron-Clearing Efficiency of Polyamine–Chelator Conjugates.** The bile-duct-cannulated rat model<sup>87–89</sup> was chosen for this initial study. In this model, chelator-promoted iron excretion is measured in both the bile and the urine. Furthermore, because the method allows for collection of multiple bile samples, the kinetics of iron excretion can be determined. In each instance, the drugs were given sc: L1 and its SPM conjugate (4 and 5) at a dose of 450  $\mu\text{mol/kg}$  and (S)-4'-(HO)-DADFT (8) and its NSPD conjugates (9 and 10) at a dose of 300  $\mu\text{mol/kg}$ , i.e., all at equivalent iron-binding capacity. L1 and its SPM conjugate form 3:1 ligand–metal complexes,<sup>72</sup> whereas the (S)-4'-(HO)-DADFT-based compounds form 2:1 ligand–metal complexes (Figure 5). As will be presented in detail below, the liver of animals given the ester 9 contained largely free acid 10. It is unlikely that the ethyl ester survives nonspecific serum esterases.

L1 (4) had an iron-clearing efficiency of  $2.2 \pm 0.9\%$  in the bile-duct-cannulated rodent; 74% of the iron was in the bile and 26% in the urine (Table 2). Despite the high intracellular accumulation of the SPM-L1 conju-

**Table 2.** Iron Clearing Efficiency of Conjugated and Unconjugated Chelators in Rodents

compd	dose, $\mu\text{mol/kg}$ , sc	iron clearing efficiency, % <sup>a</sup> (% bile/% urine)
L1 (4)	450	$2.2 \pm 0.9$ (74/26)
SPM-L1 conjugate (5)	450	$<0.5^b$ $1.8 \pm 0.9^c$ (53/47)
(S)-4'-(HO)-DADFT (8)	300	$1.1 \pm 0.6$ (93/7)
NSPD-(S)-4'-(HO)-DADFT-EE (9)	300	$13.6 \pm 3.3^d$ (97/3)
NSPD-(S)-4'-(HO)-DADFT (10)	300	$9.2 \pm 2.6^d$ (99/1)

<sup>a</sup> The compounds were given to non-iron-overloaded, bile-duct-cannulated rodents ( $n = 4$ , unless otherwise indicated), at the doses shown. The net iron excretion (after 24 h, unless otherwise indicated) was calculated by subtracting the iron excretion of control animals from the iron excretion of treated animals. Efficiency of chelation is defined as net iron excretion/total iron-binding capacity of chelator administered, expressed as a percent.

<sup>b</sup> In an initial study, iron excretion was delayed until ~18 h after drug administration. <sup>c</sup> In a subsequent assessment, the compound was given 10 h before surgery and sample collection was initiated.

<sup>d</sup> Net iron excretion was calculated after 48 h.

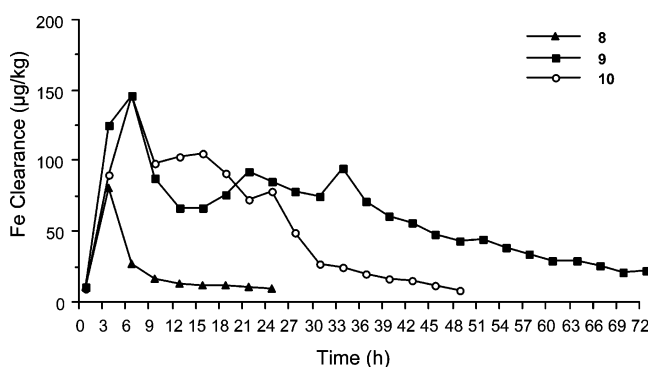


**Figure 6.** Biliary ferrokinetics of free (S)-4'-(HO)-DADFT (8) and the polyamine-vector derivatives (9 and 10) in bile duct-cannulated rats ( $n = 4/\text{compound}$ ). In all three instances, the compounds were administered sc at a dose of 300  $\mu\text{mol/kg}$ .

gate (5, Table 1), in an initial experiment with this compound, iron excretion remained at baseline levels until approximately 18 h after drug administration and the 24-h iron clearing efficiency was <0.5%. To allow for the observed delay in iron excretion, in a subsequent study the drug was given 10-h before surgery and sample collection was initiated. In this case, iron excretion remained above baseline levels from 10 to 40 h after drug administration. However, compound 5 was no more effective at clearing iron than was the parent L1 (4),  $1.8 \pm 0.9\%$ , although the mode of iron excretion changed slightly, to 53% biliary and 47% urinary (Table 2). This is consistent with the idea that once the conjugate was incorporated into the cell, its metabolism would stop after removal of the first 3-aminopropyl fragment (Figure 1). This would leave a rather large bidentate fragment to form an even larger hexacoordinate iron complex for excretion. Thus, a polyamine vector containing only cleavable aminopropyl moieties (i.e., NSPD) should compete for transport, enter the cell, be metabolized, and clear iron.

The parent (S)-4'-(HO)-DADFT ligand (8) had an iron-clearing efficiency of  $1.1 \pm 0.6\%$ ; the bile/urine ratio was 93:7. Once the NSPD vector was appended to (S)-4'-(HO)-DADFT, providing conjugate 10, the efficiency increased to  $9.2 \pm 2.6\%$ ; this efficacy increased further, to  $13.6 \pm 3.3\%$ , in the case of the corresponding ester (9). The modes of iron excretion were similar to those

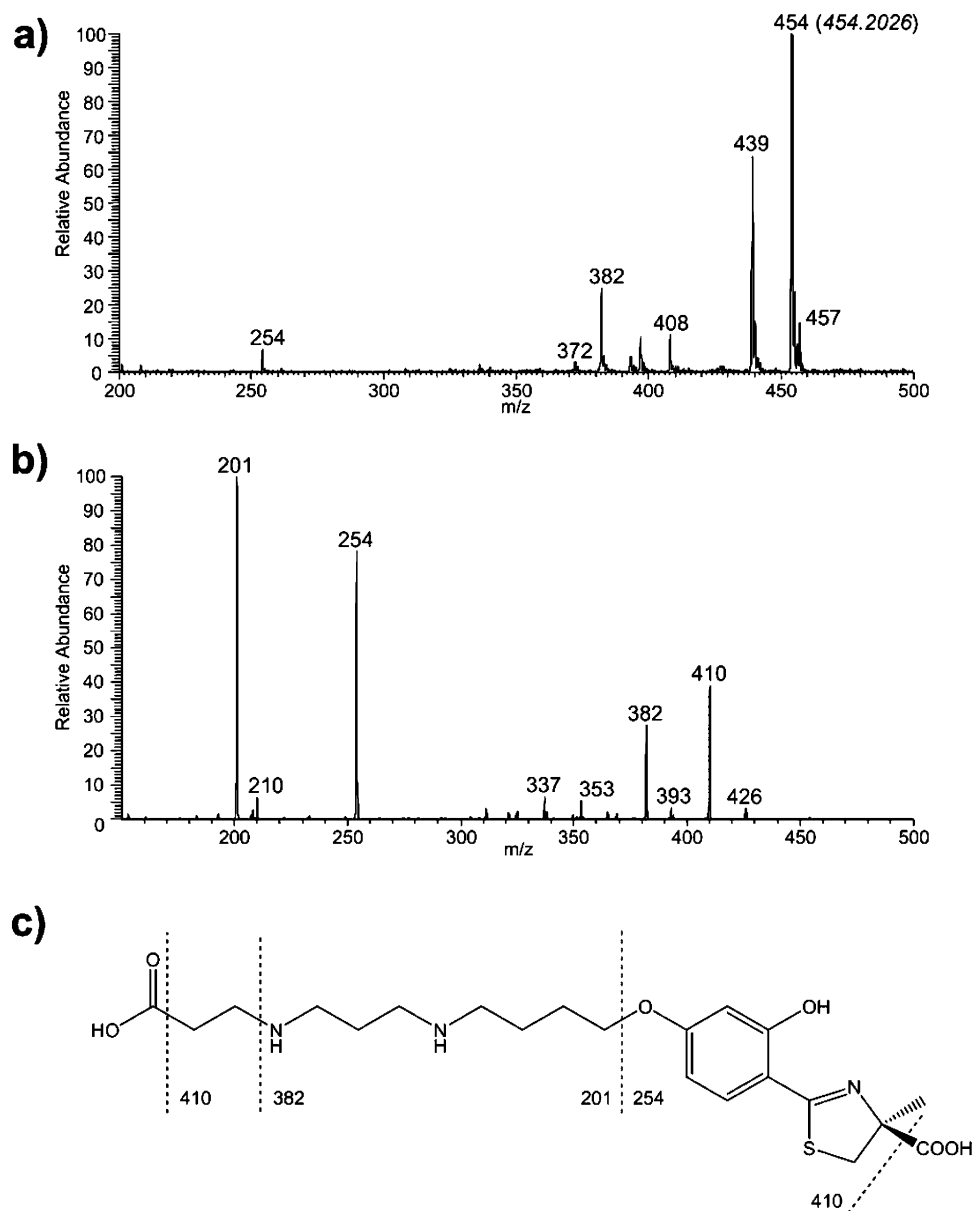


**Figure 7.** Identification of metabolite **36** of **10** by ESI mass spectrometry and MS/MS. (a) ESI-MS: Full-scan MS of the liver extract 2-h postadministration of **10**. Accurate mass for the molecular ion of the metabolite is given in italics and only matches to  $C_{21}H_{31}N_3O_6S + H^+$  (calcd 454.2012,  $\Delta = +3.1$  ppm) within 10 ppm accuracy, when the following search limits in elemental composition are set:  $C \leq 24$ ,  $H \leq 40$ ,  $N \leq 4$ ,  $O \leq 6$  and  $S \leq 1$ ; (b) MS/MS: Product-ion spectrum (CID) from  $m/z$  454; (c) Putative origin of MS/MS fragment ions from the protonated metabolite **36**.

of the parent compound **8**. However, the profound difference in the ferrokinetics associated with the polyamine-vectored (*S*)-4'-(HO)-DADFTs (**9** and **10**) vs free (*S*)-4'-(HO)-DADFT (**8**) is noteworthy (Figure 6). Both of the NSPD conjugates (**9** and **10**) elicited protracted biliary iron clearance. The ligand-induced iron clearance was essentially back to baseline 9 h after single-dose administration of **8**. In the case of the conjugate acid **10**, the return to baseline was not until 48 h after drug administration. In the case of the ester **9**, the iron excretion had not returned to baseline even after 72 h, at which time the animals were euthanized. This behavior is in keeping with the metabolic profile of the conjugates, which is presented below.

**Oxidative Deamination.** In animals treated with either NSPD-(*S*)-4'-(HO)-DADFT conjugate (ester **9** or acid **10**), the predominant metabolic product found in

the liver was the dicarboxylic acid **36** (Figure 3). This acid, the protonated molecule at  $m/z$  454, was identified using mass spectrometry (Figure 7). We also observed the corresponding lower homologue, dicarboxylic acid **37**,  $[M + H]^+$  at  $m/z$  382 (Figure 7).

Product **36** could have resulted from the action of PAO<sup>90,91</sup> or diamine oxidase<sup>91</sup> on the polyamine conjugate to first produce the corresponding terminal aldehyde. In turn, aldehyde dehydrogenase would convert this to the acid. Although there is certainly precedent for both reactions, the identity of the active enzyme(s), PAO and/or diamine oxidase, remains to be determined. The level of this metabolite is somewhat surprising and will be a major consideration in future assessments of the toxicity profile of this system. The stability of this molecule to spontaneous decomposition to acrylic acid remains to be determined. In fact, the stability of the

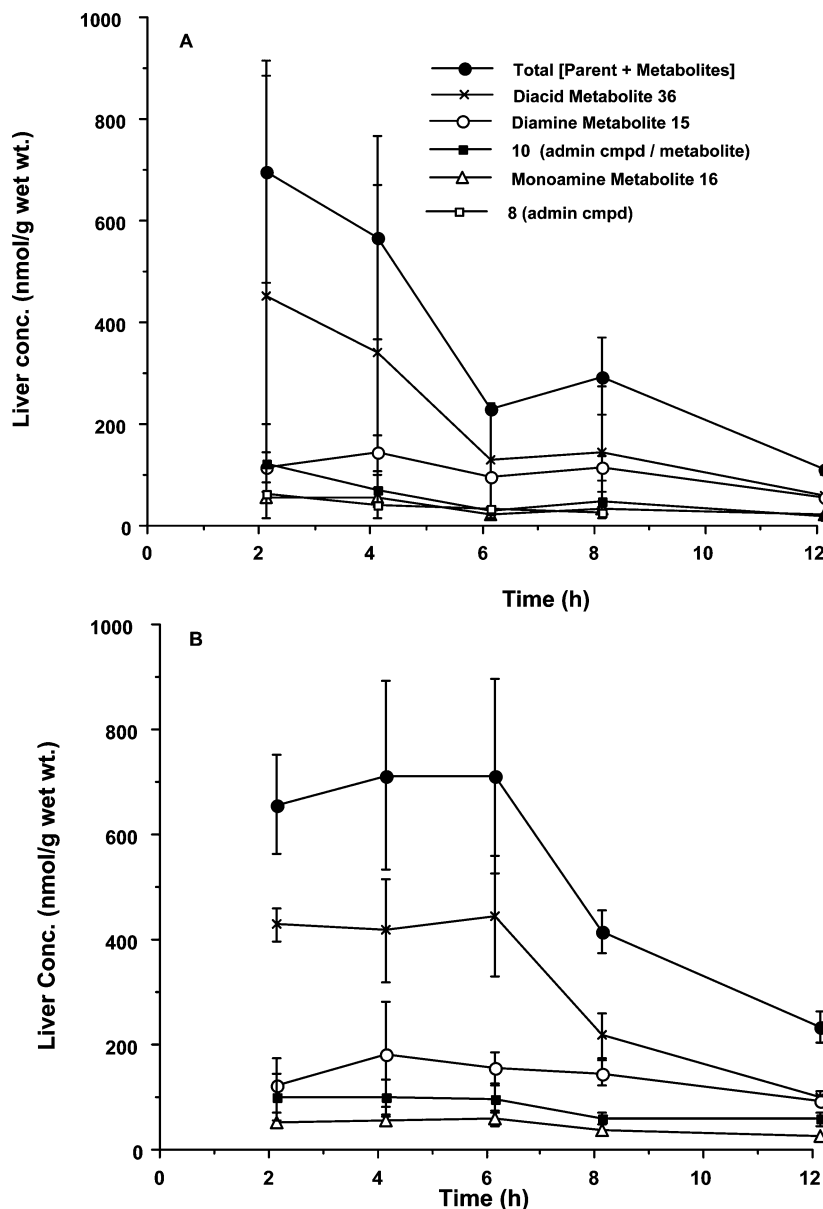


**Figure 8.** Hepatic concentrations of NSPD-(S)-4'-(HO)-DADFT and its metabolites in rats treated with NSPD-(S)-4'-(HO)-DADFT (**10**) (panel A,  $n = 5$  animals for the 2- and 4-h time points,  $n = 4$  for the 8-h time point, and  $n = 1$  for the 6- and 12-h time points). For comparison, in panel A, the concentrations of (S)-4'-(HO)-DADFT (**8**) in rats administered the compound under the same conditions<sup>46</sup> is shown for the same time points. In each case, the rats were given the compound sc at a dose of 300  $\mu\text{mol/kg}$ . In panel B, rats were treated sc with 300  $\mu\text{mol/kg}$  of NSPD-(S)-4'-(HO)-DADFT-EE (**9**) ( $n = 4$  animals for the 2- and 4-h time points;  $n = 3$  for the 6-, 8-, and 12-h time points).<sup>97</sup> No detectable ester was observed in the livers of the rats given the ester **9**. We believe that the ester was cleaved by nonspecific esterases within the tissue, as **10** is present as a major metabolite of **9**.

natural homologues, such as spermic acid, and their role in polyamine toxicity still remain somewhat controversial.<sup>91</sup>

**Metabolic Profile of Polyamine Conjugates.** In these studies, rodents were given the test drug (either **9** or **10**) sc at a dose of 300  $\mu\text{mol/kg}$  and were sacrificed at 2, 4, 6, 8, and 12 h after dosing. The liver was excised, homogenized, and analyzed by HPLC. To facilitate the analysis, both putative deaminopropylated metabolic products, diamine **15** and monoamine **16** (Figure 3), were synthesized as described above to serve as standards (Schemes 4 and 5). The metabolic fates and tissue levels of **9** and **10** are summarized in Figures 3 and 8; the tissue levels are compared to those obtained for the parent compound, (S)-4'-(HO)-DADFT (**8**),<sup>46</sup> under the same dosing conditions.

The metabolic profile of the NSPD-(S)-4'-(HO)-DADFT conjugates was similar to that observed with DENSPM (Figure 1), stepwise deaminopropylation (Figure 3, right);<sup>49,51</sup> however, there are differences (Figure 3, left, and Figure 8). After administration of either the ester **9** or the acid **10**, both deaminopropylated products **15** and **16** were identified in the HPLC chromatogram. Whereas the acid **10** was detected in the livers of rats given either **10** (Figure 8A) or ester **9** (Figure 8B), no detectable ester was observed in the livers of the rats given the ester **9**. We believe that the ester was cleaved by nonspecific esterases within the tissue, as **10** is present as a major metabolite of **9** (Figure 8B). This is consistent with the results in cell culture. Interestingly, the dicarboxylic acid metabolites **36** and **37** were also detected in the chromatograms. In fact, the dicarboxylic

acid **36** was the major form of the drug in the liver when either ester **9** or acid **10** was administered to the rodents. Although these diacids were not assembled as standards, their identities were verified by mass spectrometry.

As shown in Figure 8A, the metabolites of **10** represent the predominant form of this conjugate in liver tissue. The intact drug conjugate **10** itself never achieves levels above 150  $\mu\text{M}$ ; neither does the parent compound (*S*)-4'-(HO)-DADFT (**8**), when administered as such, or the monoamine metabolite **16**. However, the diamine **15** and the putative diacid **36** attained levels of  $100 \pm 24$  and  $436 \pm 123$   $\mu\text{M}$ , respectively, 2 h after drug dosing. Thus, the total ligand concentration ([metabolites **15**, **16**, and **36**] + [administered compound **10**]) rose to a level of nearly 700  $\mu\text{M}$ . Even 12 h after dosing, the total ligand concentration was approximately 100  $\mu\text{M}$ . Whereas the levels of administered compound **10** and monoamine and diamine metabolites **16** and **15** remained fairly constant over 8 h, the concentration of diacid metabolite **36** dropped substantially over this time period.

The overall behavior of ester **9** was somewhat different from that of the acid, achieving and maintaining higher levels of metabolites (Figure 8B). As discussed above, no administered compound (**9**) was found in liver tissue, even at 2 h after drug administration. The metabolically derived hydrolysis product, acid conjugate **10**, attained a concentration of roughly 100  $\mu\text{M}$  at 2 h and maintained this level for 12 h. Once again, the monoamine metabolite **16** never rose above 50  $\mu\text{M}$ . The diamine metabolite **15** achieved levels of approximately 150  $\mu\text{M}$  at 2 h and sustained this concentration for 8 h; the level had diminished to about 100  $\mu\text{M}$  by 12 h. Similar to the behavior with **10**, the diacid metabolite **36** was quite prominent, achieving levels of nearly 450  $\mu\text{M}$  at 2 h and diminishing to just under 100  $\mu\text{M}$  by 12 h after dosing. Thus, 8 h after drug administration, the total ligand concentration ([metabolites **10**, **15**, **16**, and **36**] in the livers of the animals given the ester conjugate **9** is greater than in the livers of the animals given the acid conjugate **10** ( $P = 0.02$ , Student's *t*-test).

## Conclusion

The data further support the utility of polyamines as vectors for the intracellular transport of chelators and underscore the importance of charge in polyamine chelator conjugate design. Neutral cargo fragments, such as L1, terephthalate methyl ester, and (*S*)-4'-(HO)-DADFT ethyl ester, are imported effectively, whereas the corresponding negatively charged carboxylate species, terephthalate and (*S*)-4'-(HO)-DADFT carboxylate, are not. The (*S*)-4'-(HO)-DADFT ethyl ester polyamine conjugate, once imported into the cell, is hydrolyzed to the corresponding free acid. Thus, the polyamine transport apparatus can be utilized to vector negatively charged carboxylate ligands simply by masking the carboxylate as an esterase-labile ester. Such conjugates make it possible to achieve millimolar levels of chelator intracellularly.

The metabolic profile in rodents suggested that a substantial fraction of the drug was oxidatively deaminated to the terminal acid, which could easily collapse

to acrylic acid and the corresponding amine. This is a significant observation with regard to future design strategies.

In rodents, the polyamine-(*S*)-4'-(HO)-DADFT conjugates, both the acid and the ester, significantly outperformed the parent ligand at iron clearance. Interestingly, the ester presented a very protracted iron clearing profile, even though the data collected from liver samples suggested that the ester itself was very short-lived and quickly hydrolyzed to the acid. The use of alternative, less labile esters is under investigation.

## Experimental Section

Desferrioxamine B in the form of the methanesulfonate salt, Desferal (**3**) (Novartis Pharma AG, Basel, Switzerland), was obtained from a hospital pharmacy. 1,2-Dimethyl-3-hydroxypyridin-4-one (L1, **4**) was a generous gift from Dr. H. H. Peter (Ciba-Geigy, Basel). Compounds **1**,<sup>92</sup> **2**,<sup>48</sup> **5**,<sup>72</sup> and **8**<sup>41</sup> were synthesized using methods published by this laboratory. 4-Hydroxy-2-methoxybenzaldehyde (**28**) was obtained from Lancaster Synthesis, Inc., Pelham, NH. Reagents were purchased from Aldrich Chemical Co. (Milwaukee, WI), and Fisher Optima-grade solvents were routinely used. Organic extracts were dried with sodium sulfate. Sodium hydride reactions were run in distilled DMF under an inert atmosphere, and THF was distilled from sodium and benzophenone. Distilled solvents and glassware that had been presoaked in 3 N HCl for 15 min were employed in reactions involving chelators. Silica gel 70–230 from Fisher Scientific was utilized for column chromatography, and silica gel 32–63 from Selecto Scientific, Inc. (Suwanee, GA) was used for flash column chromatography. Sephadex LH-20 was obtained from Amersham Biosciences (Piscataway, NJ), and AG1-X8 (hydroxide form) anion-exchange resin from Bio-Rad Laboratories, Inc. (Hercules, CA) was employed for ion exchange chromatography. Melting points are uncorrected. Optical rotations were run at 589 nm (sodium D line) utilizing a Perkin-Elmer 341 polarimeter with *c* as g of compound/100 mL of solution. NMR spectra were obtained at 300 MHz (<sup>1</sup>H) or 75 MHz (<sup>13</sup>C) on a Varian Unity 300 (not indicated), at 400 MHz (<sup>1</sup>H) or 100 MHz (<sup>13</sup>C) on a Varian Mercury-400BB, or at 600 MHz (<sup>1</sup>H) on a Bruker Avance. Chemical shifts ( $\delta$ ) for <sup>1</sup>H spectra are given in parts per million downfield from tetramethylsilane for organic solvents (CDCl<sub>3</sub> not indicated) or sodium 3-(trimethylsilyl)propionate-2,2,3,3-*d*<sub>4</sub> for D<sub>2</sub>O. Chemical shifts ( $\delta$ ) for <sup>13</sup>C spectra are given in parts per million referenced to 1,4-dioxane ( $\delta$  67.19) in D<sub>2</sub>O or to the residual solvent resonance in CDCl<sub>3</sub> ( $\delta$  77.16) or CD<sub>3</sub>OD ( $\delta$  49.00). Coupling constants (*J*) are in hertz. The base peaks are reported for the ESI-FTICR mass spectra. Elemental analyses were performed by Atlantic Microlabs (Norcross, GA).

Male Sprague–Dawley rats were obtained from Harlan Sprague–Dawley (Indianapolis, IN). Nalgene metabolic cages, rat jackets, and fluid swivels were purchased from Harvard Bioscience (South Natick, MA). Intramedic polyethylene tubing (PE 50) and surgical supplies were procured from Fisher Scientific (Pittsburgh, PA). Atomic absorption (AA) measurements were made on a Perkin-Elmer model 5100 PC (Norwalk, CT).

**N<sup>1</sup>-(4-Carbomethoxy)benzoylspermine Trihydrochloride (6)**. A solution of **13** (0.332 g, 0.500 mmol) in CH<sub>3</sub>OH (5 mL) and concentrated HCl (1.25 mL) was stirred at room temperature for 12 h. The reaction mixture was concentrated to dryness, and 0.199 g (84%) of **6** was obtained as a white solid: <sup>1</sup>H NMR (D<sub>2</sub>O)  $\delta$  1.70–1.92 (m, 4 H), 1.99–2.17 (m, 4 H), 3.06–3.22 (m, 10 H), 3.55 (t, 2 H, *J* = 6.6), 3.98 (s, 3 H), 7.87 (d, 2 H, *J* = 8.7), 8.14 (d, 2 H, *J* = 8.7); <sup>13</sup>C NMR (D<sub>2</sub>O)  $\delta$  23.42, 23.45, 24.38, 26.30, 37.21, 37.36, 45.19, 45.85, 47.57, 47.66, 53.49, 127.90, 130.30, 133.01, 138.14, 168.92, 170.58; HRMS *m/z* calcd for C<sub>19</sub>H<sub>33</sub>N<sub>4</sub>O<sub>3</sub> 365.2552 (M + H, free amine), found 365.2556.

**N<sup>1</sup>-(4-Carboxy)benzoylspermine Trihydrochloride (7)**. Freshly distilled TFA (5 mL) was added to **14** (0.326 g, 0.501

mmol) in 5 mL of dry  $\text{CH}_2\text{Cl}_2$  (5 mL) with ice bath cooling, and the reaction mixture was stirred at 0 °C for 1 h and at room temperature for 1 h. Solvents were removed under vacuum, and the residue was dissolved in  $\text{H}_2\text{O}$  (1 mL). The solution was loaded onto ion-exchange resin; elution with 1 N HCl gave 0.168 g (73%) of **7** as a white solid:  $^1\text{H}$  NMR ( $\text{D}_2\text{O}$ )  $\delta$  1.72–1.85 (m, 4 H), 1.96–2.14 (m, 4 H), 3.04–3.18 (m, 10 H), 3.53 (t, 2 H,  $J = 6.6$ ), 7.82 (d, 2 H,  $J = 8.4$ ), 8.03 (d, 2 H,  $J = 8.4$ );  $^{13}\text{C}$  NMR ( $\text{D}_2\text{O}$ )  $\delta$  23.42, 24.37, 26.31, 26.85, 37.18, 37.29, 45.16, 45.78, 47.52, 47.63, 127.91, 130.45, 134.37, 138.04, 170.91, 174.76; HRMS  $m/z$  calcd for  $\text{C}_{18}\text{H}_{31}\text{N}_4\text{O}_3$  351.2396 (M + H, free amine), found 351.2407.

**$N^1$ -(4-Carbomethoxy)benzoyl- $N^4$ , $N^9$ , $N^{12}$ -tris(*tert*-butoxycarbonyl)spermine (13).** 1,1'-Carbonyldiimidazole (0.162 g, 1.00 mmol) was added to a solution of **12** (0.180 g, 1.00 mmol) in  $\text{CH}_2\text{Cl}_2$  (5 mL). After stirring for 1 h, the solution was cooled to 0 °C, and **11** (0.502 g, 0.999 mmol) in  $\text{CH}_2\text{Cl}_2$  (3 mL) was added. The solution was stirred for 15 h (0 °C to room temperature) and was washed with 2% NaOH (20 mL),  $\text{H}_2\text{O}$ , and saturated NaCl. After solvent was removed by rotary evaporation, flash chromatography, eluting with 5%  $\text{CH}_3\text{OH}/\text{CHCl}_3$ , gave 0.510 g (77%) of **13**:  $^1\text{H}$  NMR  $\delta$  1.40–1.78 (s + m, 35 H), 3.05–3.50 (m, 12 H), 3.94 (s, 3 H), 7.91–8.20 (m, 4 H);  $^{13}\text{C}$  NMR  $\delta$  26.02, 27.54, 28.26, 28.39, 29.04, 35.20, 37.48, 37.75, 43.28, 43.89, 44.29, 46.28, 46.80, 52.32, 78.98, 79.64, 80.12, 127.19, 129.73, 132.41, 138.64, 155.51, 156.06, 156.83, 166.20, 166.51. Anal. ( $\text{C}_{34}\text{H}_{56}\text{N}_4\text{O}_9 \cdot 0.5\text{H}_2\text{O}$ ) C, H, N.

**$N^1$ -(4-Carboxy)benzoyl- $N^4$ , $N^9$ , $N^{12}$ -tris(*tert*-butoxycarbonyl)spermine (14).** A solution of **13** (0.664 g, 0.999 mmol) in 1 N NaOH (10 mL) and  $\text{CH}_3\text{OH}$  (10 mL) was stirred for 12 h. The reaction mixture was acidified to pH 2 with 1 N HCl and was extracted with EtOAc (4  $\times$  10 mL). The organic phase was washed with  $\text{H}_2\text{O}$  and saturated NaCl and was dried over  $\text{MgSO}_4$ . Solvent was removed under reduced pressure to generate 0.521 g (80%) of **14** as an oil:  $^1\text{H}$  NMR  $\delta$  1.30–1.94 (s + m, 35 H), 3.05–3.52 (m, 12 H), 5.27 (br s, 1 H), 7.92–8.28 (m, 4 H);  $^{13}\text{C}$  NMR  $\delta$  26.11, 27.56, 28.54, 36.18, 37.59, 43.51, 44.06, 44.41, 46.90, 79.18, 79.80, 80.39, 127.25, 130.25, 132.54, 138.91, 156.24, 156.92, 166.75, 169.30, 174.82; HRMS  $m/z$  calcd for  $\text{C}_{33}\text{H}_{54}\text{N}_4\text{NaO}_9$  673.3788 (M + Na), found 673.3735.

**Ethyl (S)-4,5-Dihydro-2-[2-hydroxy-4-(12-amino-5,9-diazadodecyloxy)phenyl]-4-methyl-4-thiazolecarboxylate Trihydrochloride (9).** Acetyl chloride (0.235 g, 2.99 mmol) was added to **25** (0.383 g, 0.499 mmol) in  $\text{CH}_3\text{CH}_2\text{OH}$  (10 mL) with ice cooling. The reaction was warmed to room temperature and was stirred overnight. Concentration under high vacuum led to 0.188 g (65%) of **9** as a white solid:  $[\alpha]_D^{26} +67.7^\circ$  (c 0.62,  $\text{H}_2\text{O}$ );  $^1\text{H}$  NMR ( $\text{D}_2\text{O}$ )  $\delta$  1.29 (t, 3 H,  $J = 7.2$ ), 1.81 (s, 3 H), 1.83–1.96 (m, 4 H), 2.02–2.20 (m, 4 H), 3.04–3.25 (m, 10 H), 3.62 (d, 1 H,  $J = 12.0$ ), 4.01 (d, 1 H,  $J = 12.3$ ), 4.17 (t, 3 H,  $J = 5.8$ ), 4.30 (q, 2 H,  $J = 7.2$ ), 6.59 (d, 1 H,  $J = 2.4$ ), 6.67 (dd, 1 H,  $J = 9.0$ , 2.4), 7.65 (d, 1 H,  $J = 9.0$ );  $^{13}\text{C}$  NMR ( $\text{D}_2\text{O}$ )  $\delta$  13.79, 23.05, 23.30, 24.34, 25.96, 29.27, 37.14, 39.27, 45.00, 45.26, 45.33, 48.13, 64.57, 68.76, 76.83, 102.00, 107.11, 109.81, 134.44, 159.47, 161.46, 167.21, 172.88; HRMS  $m/z$  calcd for  $\text{C}_{23}\text{H}_{39}\text{N}_4\text{O}_4\text{S}$  467.2692 (M + H, free amine), found 467.2685.

**(S)-4,5-Dihydro-2-[2-hydroxy-4-(12-amino-5,9-diazadodecyloxy)phenyl]-4-methyl-4-thiazolecarboxylic Acid Trihydrochloride (10).** Freshly distilled TFA (5 mL) in  $\text{CH}_2\text{Cl}_2$  (5 mL) was added dropwise to **26** (0.370 g, 0.501 mmol) in  $\text{CH}_2\text{Cl}_2$  (5 mL) with ice bath cooling. The mixture was stirred at room temperature for 30 min, and solvents were removed by rotary evaporation. The solid was passed through an ion-exchange resin, eluting with 1 N HCl to yield 0.233 g (85%) of **10**:  $[\alpha]_D^{26} +50.8^\circ$  (c 0.295,  $\text{H}_2\text{O}$ ); 600 MHz  $^1\text{H}$  NMR ( $\text{D}_2\text{O}$ ), see Figure 4;  $^{13}\text{C}$  NMR ( $\text{D}_2\text{O}$ )  $\delta$  23.04, 23.30, 24.35, 25.94, 37.15, 39.18, 44.92, 45.00, 45.27, 45.34, 48.13, 68.86, 75.64, 101.95, 106.23, 110.22, 134.96, 161.39, 168.10, 174.69, 182.87; HRMS  $m/z$  calcd for  $\text{C}_{21}\text{H}_{34}\text{N}_4\text{O}_4\text{S}$  439.2379 (M + H, free amine), found 439.2374.

**$N^1$ , $N^4$ -Bis(*tert*-butoxycarbonyl)- $N^7$ -(mesitylenesulfonyl)-norspermidine (19).** Sodium hydroxide (9.81 g, 0.245 mol) in 9% aqueous  $\text{CH}_3\text{CH}_2\text{OH}$  (220 mL) and Raney 2800 nickel

(6.66 g) were successively added to a solution of **17** (8.54 g, 26.1 mmol) in  $\text{CH}_3\text{CH}_2\text{OH}$  (45 mL) in a 500-mL Parr bottle. After hydrogenation was carried out at 50–55 psi for 12 h, the suspension was filtered, and the solids were washed with 95%  $\text{CH}_3\text{CH}_2\text{OH}$  (200 mL). Solvents were removed in vacuo, and **18** was diluted with  $\text{H}_2\text{O}$  (125 mL) and  $\text{CH}_2\text{Cl}_2$  (100 mL). A solution of mesitylenesulfonyl chloride (6.02 g, 27.5 mmol) in  $\text{CH}_2\text{Cl}_2$  (100 mL) was added dropwise to the biphasic mixture with ice bath cooling. The mixture was stirred at room temperature for 12 h. The layers were separated, and the aqueous layer was extracted further with  $\text{CH}_2\text{Cl}_2$  (3  $\times$  150 mL). Organic extracts were washed with  $\text{H}_2\text{O}$  (2  $\times$  225 mL) and saturated NaCl (2  $\times$  225 mL), and solvent was removed by rotary evaporation. Flash chromatography, eluting with 2:1 hexanes/EtOAc, afforded 11.38 g (85%) of **19** as a white foam:  $^1\text{H}$  NMR  $\delta$  1.42 and 1.43 (2 s, 18 H), 1.55–1.69 (m, 4 H), 2.29 (s, 3 H), 2.65 (s, 6 H), 2.82–2.92 (m, 2 H), 3.01–3.29 (m, 6 H), 4.64 and 5.17 (2 br s, 1 H), 6.03 (br s, 1 H), 6.93 (s, 2 H);  $^{13}\text{C}$  NMR  $\delta$  20.98, 23.03, 28.45, 28.51, 28.94, 37.83, 39.16, 43.01, 44.26, 79.17, 80.40, 131.98, 134.77, 138.94, 141.74, 156.05, 156.41. Anal. ( $\text{C}_{25}\text{H}_{43}\text{N}_3\text{O}_6\text{S}$ ): C, H, N.

**$N^1$ -(4-Benzoyloxybutyl)- $N^4$ , $N^7$ -bis(*tert*-butoxycarbonyl)- $N^1$ -(mesitylenesulfonyl)norspermidine (20).** Sodium hydride (60%, 1.18 g, 29.5 mmol) was added in portions to **19** (11.38 g, 22.1 mmol) in DMF (125 mL) with ice bath cooling, and the mixture was stirred at 0 °C for 45 min and at room temperature for 1 h. A solution of benzyl 4-bromobutyl ether (90%, 6.02 g, 22.3 mmol) in DMF (40 mL) was added to the reaction mixture over 30 min. After stirring for 19 h, quenching with  $\text{H}_2\text{O}$  (30 mL) at 0 °C was performed, and solvents were removed under high vacuum. The concentrate was dissolved in  $\text{CHCl}_3$  (500 mL), which was washed with  $\text{H}_2\text{O}$  (2  $\times$  300 mL) and saturated NaCl (2  $\times$  300 mL); solvent was removed in vacuo. Flash chromatography, eluting with 3:1 hexanes/EtOAc, gave 11.71 g (78%) of **20** as a colorless oil:  $^1\text{H}$  NMR  $\delta$  1.44 (s, 18 H), 1.4–1.5 (m, 2 H), 1.5–1.6 (m, 4 H), 1.65–1.77 (m, 2 H), 2.28 (s, 3 H), 2.58 (s, 6 H), 2.95–3.22 (m, 10 H), 3.35 (t, 2 H,  $J = 5.9$ ), 4.43 (s, 2 H), 4.73 and 5.25 (2 br s, 1 H), 6.92 (s, 2 H), 7.25–7.38 (m, 5 H);  $^{13}\text{C}$  NMR  $\delta$  21.26, 23.02, 24.45, 27.10, 28.62, 28.66, 37.51, 43.52, 44.40, 45.70, 69.79, 73.11, 80.00, 125.98, 127.79, 128.58, 132.14, 133.48, 138.63, 140.30, 142.57, 149.55, 156.30. Anal. ( $\text{C}_{36}\text{H}_{57}\text{N}_3\text{O}_7\text{S}$ ): C, H, N.

**$N^1$ -(4-Hydroxybutyl)- $N^1$ , $N^4$ , $N^7$ -tris(*tert*-butoxycarbonyl)norspermidine (22).** Hydrogen bromide (30% in HOAc, 105 mL) was added dropwise to a solution of **20** (5.57 g, 8.24 mmol) and phenol (9.03 g, 96.0 mmol) in  $\text{CH}_2\text{Cl}_2$  (75 mL) at 0 °C. After the reaction mixture was stirred for 12 h while being warmed to room temperature under a  $\text{N}_2$  balloon,  $\text{H}_2\text{O}$  (125 mL) was added under ice bath cooling, and the layers were separated. After additional extraction with  $\text{CH}_2\text{Cl}_2$  (3  $\times$  150 mL), the aqueous portion was evaporated under high vacuum, and **21** was dissolved in 5% aqueous THF (105 mL). Triethylamine (6.18 g, 61.1 mmol) and di-*tert*-butyl dicarbonate (6.02 g, 27.6 mmol) in THF (60 mL) were successively added with ice bath cooling, and the reaction mixture was stirred for 12 h at room temperature. Following solvent removal by rotary evaporation, the residue was dissolved in EtOAc (500 mL), which was washed with 250 mL portions of  $\text{H}_2\text{O}$ , 0.25 M citric acid,  $\text{H}_2\text{O}$ , 1 M  $\text{Na}_2\text{CO}_3$ ,  $\text{H}_2\text{O}$ , and saturated NaCl. After solvent was removed in vacuo, flash chromatography, eluting with 4%  $\text{CH}_3\text{OH}/\text{CHCl}_3$ , furnished 2.46 g (59%) of **22** as a colorless oil:  $^1\text{H}$  NMR  $\delta$  1.44, 1.45, and 1.46 (3 s, 27 H), 1.5–1.8 (m, 9 H), 3.02–3.34 (m, 10 H), 3.67 (t, 2 H,  $J = 5.9$ ), 4.78 and 5.27 (2 br s, 1 H);  $^{13}\text{C}$  NMR  $\delta$  25.20, 27.84, 28.57, 28.60, 28.61, 29.82, 37.72, 44.10, 45.01, 47.01, 62.57, 79.57, 155.75, 156.16, 174.84; HRMS  $m/z$  calcd for  $\text{C}_{25}\text{H}_{50}\text{N}_3\text{O}_7$  504.3648 (M + H), found 504.3640.

**$N^1$ , $N^4$ , $N^7$ -Tris(*tert*-butoxycarbonyl)- $N^1$ -[4-(tosyloxy)butyl]norspermidine (23).** *p*-Toluenesulfonyl chloride (0.570 g, 2.99 mmol) in  $\text{CH}_2\text{Cl}_2$  (2 mL) was added to **22** (1.00 g, 1.99 mmol) in  $\text{CH}_2\text{Cl}_2$  (3 mL) followed by triethylamine (570  $\mu\text{L}$ , 4.09 mmol) at 0 °C. The reaction was stirred at room temperature for 12 h and was concentrated. The residue was dissolved in EtOAc (100 mL), which was washed with 50-mL portions

of 8% NaHCO<sub>3</sub>, 0.5 M citric acid, H<sub>2</sub>O, and saturated NaCl. Solvent removal and flash chromatography, eluting with 3% CH<sub>3</sub>OH/CH<sub>2</sub>Cl<sub>2</sub>, afforded 1.20 g (92%) of **23** as an oil: <sup>1</sup>H NMR δ 1.40–1.85 (m, 35 H), 2.30 (s, 3 H), 3.04–3.30 (m, 10 H), 4.03 (t, 2 H, *J* = 6.0), 5.28 (br s, 1 H), 7.35 (d, 2 H, *J* = 8.1), 7.75 (d, 2 H, *J* = 8.4); <sup>13</sup>C NMR δ 21.28, 21.59, 22.86, 23.12, 25.81, 26.20, 26.82, 30.90, 31.18, 34.41, 37.00, 44.35, 53.53, 54.18, 80.19, 125.72, 125.83, 127.82, 128.84, 129.83, 133.06, 140.15, 141.98, 149.30. Anal. (C<sub>32</sub>H<sub>55</sub>N<sub>3</sub>O<sub>9</sub>S): C, H, N.

**Ethyl (S)-2-(2,4-Dihydroxyphenyl)-4,5-dihydro-4-methyl-4-thiazolecarboxylate (24)**. Iodoethane (7.02 g, 45.0 mmol) and DIEA (5.81 g, 45.0 mmol) were successively added to **8** (6.33 g, 25.0 mmol) in DMF (290 mL), and the solution was stirred at room temperature for 15 h. After solvent removal under high vacuum, the residue was treated with 1:1 0.5 M citric acid/saturated NaCl (250 mL) and was extracted with EtOAc (3 × 150 mL). The combined extracts were washed with 250-mL portions of 0.25 M citric acid, 1% NaHSO<sub>3</sub>, H<sub>2</sub>O, and saturated NaCl, and solvent was evaporated. Purification by flash column chromatography using 1:3:6 EtOAc/hexanes/CH<sub>2</sub>Cl<sub>2</sub> furnished 6.72 g (96%) of **24** as a light yellow oil: [α]<sub>D</sub><sup>25</sup> +50.8° (c 1.26, CHCl<sub>3</sub>); <sup>1</sup>H NMR δ 1.30 (2 t, 3 H, *J* = 7.1), 1.66 (s, 3 H), 3.19 (d, 1 H, *J* = 11.3), 3.83 (d, 1 H, *J* = 11.3), 4.25 (q, 2 H, *J* = 7.1), 6.37 (dd, 1 H, *J* = 8.6, 2.4), 6.44 (d, 1 H, *J* = 2.4), 7.27 (d, 1 H, *J* = 8.6) 12.5 (br s, 1 H); <sup>13</sup>C NMR δ 16.92, 27.32, 42.71, 64.88, 85.94, 105.95, 110.20, 112.89, 135.04, 163.20, 164.06, 175.88. Anal. (C<sub>13</sub>H<sub>15</sub>NO<sub>4</sub>S) C, H, N.

**Ethyl (S)-4,5-Dihydro-2-[2-hydroxy-4-[12-(*tert*-butoxycarbonylamino)-5,9-bis(*tert*-butoxycarbonyl)-5,9-diazadodecyloxy]phenyl]-4-methyl-4-thiazolecarboxylate (25)**. A mixture of **23** (1.67 g, 2.54 mmol), **24** (0.751 g, 2.67 mmol), and freshly prepared 0.20 M sodium ethoxide in CH<sub>3</sub>CH<sub>2</sub>OH (8 mL, 1.6 mmol) was stirred at 60 °C for 15 h. After the white solid was filtered, the filtrate was concentrated by rotary evaporation. The residue was dissolved in CHCl<sub>3</sub> (100 mL) and was washed with H<sub>2</sub>O and saturated NaCl. Solvent removal and column chromatography on silica gel, eluting with 5% EtOAc/CH<sub>2</sub>Cl<sub>2</sub>, gave 1.31 g (67%) of **25** as a pale yellow oil: [α]<sub>D</sub><sup>25</sup> +17.0° (c 1.00, CHCl<sub>3</sub>); <sup>1</sup>H NMR δ 1.30 (t, 3 H, *J* = 7.2), 1.4–1.8 (s + m, 35 H), 3.02–3.33 (m + d, 11 H, *J* = 11.4), 3.83 (d, 1 H, *J* = 11.1), 3.98 (t, 2 H, *J* = 5.8), 4.24 (2 q, 2 H, *J* = 7.2), 6.41 (dd, 1 H, *J* = 8.6, 2.4), 6.46 (d, 1 H, *J* = 2.4), 7.28 (d, 1 H, *J* = 6.6); <sup>13</sup>C NMR δ 14.18, 24.57, 26.42, 26.50, 28.54, 28.56, 28.58, 29.81, 37.51, 39.92, 43.67, 44.97, 46.79, 61.91, 67.78, 79.52, 79.74, 83.21, 101.39, 107.24, 109.81, 131.77, 155.58, 156.10, 161.33, 163.29, 170.87, 172.91, 182.00. Anal. (C<sub>38</sub>H<sub>62</sub>N<sub>4</sub>O<sub>10</sub>S): C, H, N.

**(S)-4,5-Dihydro-2-[2-hydroxy-4-[12-(*tert*-butoxycarbonylamino)-5,9-bis(*tert*-butoxycarbonyl)-5,9-diazadodecyloxy]phenyl]-4-methyl-4-thiazolecarboxylic Acid (26)**. Treatment of **25** (0.383 g, 0.499 mmol) with 1 M methanolic NaOH (5 mL, 5 mmol) at room temperature for 15 h, acidification with 1 N HCl, and solvent removal in vacuo gave a pink solid. Purification using a short Sephadex LH-20 column, eluting with CH<sub>3</sub>OH, gave an iron active band, which was dried to provide 233 mg (63%) of **26** as a white solid: [α]<sub>D</sub><sup>26</sup> +8.8° (c 1.02, CH<sub>3</sub>OH); <sup>1</sup>H NMR δ 1.38–1.84 (s + m, 35 H), 3.02–3.32 (m + d, 11 H, *J* = 11.4), 3.87 (d, 1 H, *J* = 11.4), 3.98 (t, 2 H, *J* = 5.6), 6.41 (d, 1 H, *J* = 8.7), 6.48 (s, 1 H), 7.28 (d, 1 H, *J* = 6.0); <sup>13</sup>C NMR δ 24.64, 26.46, 28.57, 28.59, 28.62, 29.00, 37.34, 39.91, 45.03, 46.86, 67.79, 79.76, 79.91, 83.05, 101.48, 107.37, 109.71, 131.88, 155.74, 161.39, 162.23, 163.40, 174.85, 186.55; HRMS *m/z* calcd for C<sub>36</sub>H<sub>59</sub>N<sub>4</sub>O<sub>10</sub>S 739.3952 (M + H), found 739.3898. Anal. (C<sub>36</sub>H<sub>58</sub>N<sub>4</sub>O<sub>10</sub>S·0.5H<sub>2</sub>O): C, H, N.

**(S)-4,5-Dihydro-2-[2-hydroxy-4-(8-amino-5-azaocetyl-oxo)phenyl]-4-methyl-4-thiazolecarboxylic Acid Bis(trifluoroacetate) (15)**. Trifluoroacetic acid (2 mL) was added to **32** (0.1 g, 0.17 mmol), and the solution was stirred for 1 h at room temperature under N<sub>2</sub>. After TFA removal in vacuo, the residue was treated with CH<sub>2</sub>Cl<sub>2</sub> and CH<sub>3</sub>CH<sub>2</sub>OH. Solvent removal in vacuo produced **15** (quantitatively) as tan crystals: mp 122–124 °C; [α]<sub>D</sub><sup>25</sup> +18.8° (c 0.85, CH<sub>3</sub>OH); <sup>1</sup>H NMR (D<sub>2</sub>O) δ 1.68 (s, 3 H), 1.80–1.92 (m, 4 H), 2.09 (quintet, 2 H,

*J* = 8.1), 3.06–3.22 (m, 6 H), 3.44 (d, 1 H, *J* = 11.1), 3.84 (d, 1 H, *J* = 11.7), 4.06–4.20 (m, 2 H), 6.45 (s, 1 H), 6.50 (d, 1 H, *J* = 8.7), 7.46 (d, 1 H, *J* = 8.7); <sup>13</sup>C NMR (D<sub>2</sub>O) δ 21.42, 21.55, 22.75, 24.31, 35.56, 37.60, 43.46, 46.46, 74.46, 100.33, 104.66, 108.48, 115.35 (*J* = 290), 133.29, 159.71, 161.93 (q, *J* = 35), 166.32, 173.59, 180.80; HRMS *m/z* calcd for C<sub>18</sub>H<sub>28</sub>N<sub>3</sub>O<sub>4</sub>S 382.1800 (M + H, free amine), found 382.1808.

**N,N'-Bis(*tert*-butoxycarbonyl)-N-[4-(tosyloxy)butyl]-1,3-diaminopropane (30)**. *p*-Toluenesulfonyl chloride (0.82 g, 4.3 mmol) in CH<sub>2</sub>Cl<sub>2</sub> (5 mL) was added to **29** (1.0 g, 2.9 mmol) in CH<sub>2</sub>Cl<sub>2</sub> (5 mL) at 0 °C, followed by NEt<sub>3</sub> (0.82 mL, 5.9 mmol). The reaction mixture was stirred at room temperature under N<sub>2</sub> for 18 h and was concentrated in vacuo. The residue was diluted with EtOAc (50 mL), followed by washing with 50 mL portions of saturated NaHCO<sub>3</sub>, 0.5 M citric acid, H<sub>2</sub>O, and saturated NaCl. After solvent removal in vacuo, flash chromatography, eluting with 3% CH<sub>3</sub>OH/CH<sub>2</sub>Cl<sub>2</sub>, gave 1.15 g (80%) of **30** as a colorless viscous oil: <sup>1</sup>H NMR (CD<sub>3</sub>OD) δ 1.30–1.70 (m, 6 H), 1.43 (s, 18 H), 2.46 (s, 3 H), 2.97–3.05 (m, 2 H), 3.15 (q, 4 H, *J* = 6.6), 4.05 (t, 2 H, *J* = 6.4), 6.57 (s, 1 H), 7.44 (d, 2 H, *J* = 8.1), 7.78 (d, 2 H, *J* = 8.4); <sup>13</sup>C NMR δ 21.75, 24.44, 24.68, 26.35, 28.55, 37.53, 43.72, 44.31, 46.18, 70.20, 79.10, 79.86, 127.98, 129.98, 133.23, 144.90, 156.11. Anal. (C<sub>24</sub>H<sub>40</sub>N<sub>2</sub>O<sub>7</sub>S): C, H, N.

**Ethyl (S)-4,5-Dihydro-2-[2-hydroxy-4-[8-(*tert*-butoxycarbonylamino)-5-(*tert*-butoxycarbonyl)-5-azaocetyl-oxyl]phenyl]-4-methyl-4-thiazolecarboxylate (31)**. Sodium (0.024 g, 1.0 mmol) was introduced to CH<sub>3</sub>CH<sub>2</sub>OH (10 mL) under N<sub>2</sub>, and the solution was added to **24** (0.33 g, 1.2 mmol) and **30** (0.55 g, 1.1 mmol). The reaction mixture was heated to 80 °C for 16 h and was concentrated in vacuo. The residue was taken up in CHCl<sub>3</sub> (30 mL), which was washed with H<sub>2</sub>O (20 mL) and saturated NaCl (20 mL). After solvent was removed by rotary evaporation, column chromatography on silica gel, eluting with 5:1 hexanes/EtOAc, furnished 0.25 g (37%) of **31** a glass: [α]<sub>D</sub><sup>25</sup> +31.9° (c 0.97, CHCl<sub>3</sub>); <sup>1</sup>H NMR (CD<sub>3</sub>OD) δ 1.28 (t, 3 H, *J* = 7.2), 1.43 (s, 9 H), 1.45 (s, 9 H), 1.64 (s, 3 H), 1.64–1.80 (m, 6 H), 2.97–3.08 (m, 2 H), 3.20–3.32 (m, 5 H), 3.83 (d, 1 H, *J* = 11.4), 4.03 (t, 2 H, *J* = 6.0), 4.23 (q, 2 H, *J* = 7.2), 6.46 (s, 1 H), 6.49 (d, 1 H, *J* = 2.4), 6.59 (s, 1 H), 7.32 (d, 1 H, *J* = 9.0); <sup>13</sup>C NMR δ 14.19, 24.57, 25.35, 26.51, 28.55, 37.46, 39.93, 43.88, 46.69, 61.98, 67.77, 79.76, 83.21, 101.37, 107.26, 109.82, 131.78, 156.22, 161.33, 163.28, 170.88, 172.92, 184.05. Anal. (C<sub>30</sub>H<sub>47</sub>N<sub>3</sub>O<sub>8</sub>S): C, H, N.

**(S)-4,5-Dihydro-2-[2-hydroxy-4-[8-(*tert*-butoxycarbonylamino)-5-(*tert*-butoxycarbonyl)-5-azaocetyl-oxyl]phenyl]-4-methyl-4-thiazolecarboxylic Acid (32)**. Sodium hydroxide (1 N, 1.2 mL, 1.2 mmol) was added to **31** (0.15 g, 0.25 mmol) in CH<sub>3</sub>CH<sub>2</sub>OH (1.2 mL). The reaction was stirred at room temperature for 16 h and was concentrated under reduced pressure. The residue was treated with 1 N HCl (20 mL), followed by extraction with EtOAc (3 × 20 mL). The combined extracts were washed with H<sub>2</sub>O (30 mL) and saturated NaCl (30 mL). Solvent removal in vacuo yielded 0.11 g (77%) of **32** a viscous tan oil: [α]<sub>D</sub><sup>25</sup> +18.5° (c 0.96, CH<sub>3</sub>OH); <sup>1</sup>H NMR δ 1.44 (s, 9 H), 1.46 (s, 9 H), 1.56–1.80 (m, 6 H), 1.72 (s, 3 H), 3.04–3.30 (m, 6 H), 3.24 (d, 1 H, *J* = 11.4), 3.86 (d, 1 H, *J* = 11.4), 3.94–4.04 (m, 2 H), 5.34 (br s, 1 H), 6.42 (d, 1 H, *J* = 8.4), 6.48 (s, 1 H), 7.29 (d, 1 H, *J* = 8.4); <sup>13</sup>C NMR (CD<sub>3</sub>OD) δ 25.34, 27.49, 28.74, 28.79, 38.97, 41.41, 68.74, 79.94, 80.99, 86.50, 102.44, 107.49, 111.40, 132.48, 157.44, 158.44, 162.82, 164.34, 169.75, 180.15; HRMS *m/z* calcd for C<sub>28</sub>H<sub>43</sub>N<sub>3</sub>NaO<sub>8</sub>S 604.2668 (M + Na), found 604.2687.

**(S)-4,5-Dihydro-2-[2-hydroxy-4-(4-aminobutoxy)phenyl]-4-methyl-4-thiazolecarboxylic Acid Trifluoroacetate (16)**. Trifluoroacetic acid (5 mL) was added to **35** (0.505 g, 1.19 mmol) in CH<sub>2</sub>Cl<sub>2</sub> (5 mL) with ice bath cooling, and the solution was stirred for 1 h at 0 °C and for 1 h at room temperature. Removal of volatiles in vacuo gave a white solid, which was passed through a short Sephadex LH-20 column, eluting with 70:30 toluene/CH<sub>3</sub>OH. The iron active band was dried to provide 0.331 g (63%) of **16** as a white solid: [α]<sub>D</sub><sup>26</sup> +110.8° (c 0.48, H<sub>2</sub>O); <sup>1</sup>H NMR (CD<sub>3</sub>OD) δ 1.74 (s, 3 H), 1.77–2.03 (m, 4 H), 3.46 (d, 1 H, *J* = 12.0), 3.93 (d, 1 H, *J* = 11.7), 4.10 (t, 2 H,

$J = 5.4$ ), 6.53 (d, 1 H,  $J = 2.4$ ), 6.57 (dd, 1 H,  $J = 8.7, 2.4$ ), 7.53 (d, 1 H,  $J = 8.7$ );  $^{13}\text{C}$  NMR ( $\text{D}_2\text{O}$ )  $\delta$  24.25, 24.81, 25.93, 39.48, 39.83, 68.84, 77.68, 101.82, 106.44, 109.59, 119.88 (q,  $J = 290$ ), 134.35, 161.39, 163.54 ( $J = 35$ ), 167.13, 176.88, 179.96; HRMS  $m/z$  calcd for  $\text{C}_{15}\text{H}_{21}\text{N}_2\text{O}_4\text{S}$  325.1222 (M + H, free amine), found 325.1226.

**Ethyl (S)-4,5-Dihydro-2-[2-hydroxy-4-[4-(tert-butoxycarbonylamino)butoxy]phenyl]-4-methyl-4-thiazolecarboxylate (34).** A mixture of **24** (0.887 g, 3.15 mmol), **33** (1.03 g, 3.00 mmol), and freshly prepared 0.20 M sodium ethoxide in  $\text{CH}_3\text{CH}_2\text{OH}$  (6 mL, 1.2 mmol) was stirred at  $75^\circ\text{C}$  for 15 h. After filtration, solvent was removed by rotary evaporation. The residue was dissolved in  $\text{CHCl}_3$  (100 mL) and was washed with  $\text{H}_2\text{O}$  and saturated NaCl. Solvent removal and column chromatography on silica gel, eluting with 4% EtOAc/ $\text{CH}_2\text{Cl}_2$  gave 600 mg (55%) of **34** as a light yellow oil:  $[\alpha]_D^{26} +31.7^\circ$  (c 1.03,  $\text{CHCl}_3$ );  $^1\text{H}$  NMR (400 MHz)  $\delta$  1.29 (t, 3 H,  $J = 7.2$ ), 1.42–1.48 (m, 9 H), 1.64 (s, 3 H), 1.76–1.90 (m, 4 H), 3.12–3.39 (d + m, 3 H,  $J = 11.2$ ), 3.83 (d, 1 H,  $J = 11.2$ ), 3.99 (t, 2 H,  $J = 6.4$ ), 4.25 (dq, 2 H,  $J = 6.8, 1.2$ ), 4.61 (br s, 1 H), 6.42 (dd, 1 H,  $J = 8.7, 2.4$ ), 6.47 (d, 1 H,  $J = 2.4$ ), 7.28 (d, 1 H,  $J = 6.6$ );  $^{13}\text{C}$  NMR  $\delta$  14.16, 24.54, 25.83, 26.45, 28.49, 40.31, 46.03, 61.94, 67.75, 78.94, 79.17, 101.38, 107.20, 109.80, 131.75, 156.08, 161.30, 163.24, 170.86, 172.88. Anal. ( $\text{C}_{22}\text{H}_{32}\text{N}_2\text{O}_6\text{S}$ ): C, H, N.

**(S)-4,5-Dihydro-2-[2-hydroxy-4-[4-(tert-butoxycarbonylamino)butoxy]phenyl]-4-methyl-4-thiazolecarboxylic Acid (35).** A solution of **34** (0.212 g, 0.468 mmol) in 1 N NaOH (5 mL, 5 mmol) and  $\text{CH}_3\text{CH}_2\text{OH}$  (5 mL) was stirred overnight at room temperature. After acidification with 1 N HCl to a pH of 3, the aqueous layer was extracted with EtOAc (3  $\times$  50 mL). The organic layer was washed with  $\text{H}_2\text{O}$  and saturated NaCl and was evaporated to generate 0.125 g (63%) of **35** as a white solid:  $[\alpha]_D^{26} +19.8^\circ$  (c 0.98,  $\text{CH}_3\text{OH}$ );  $^1\text{H}$  NMR (400 MHz)  $\delta$  1.40–1.46 (m, 9 H), 1.63–1.93 (s + m, 7 H), 3.11–3.38 (d + m, 3 H,  $J = 10.8$ ), 3.82 (d, 1 H,  $J = 10.8$ ), 3.98 (t, 2 H,  $J = 6.4$ ), 4.60 (br s, 1 H), 6.28–6.53 (s + d, 2 H,  $J = 8.8$ ), 7.28 (d, 1 H,  $J = 8.8$ );  $^{13}\text{C}$  NMR  $\delta$  24.53, 26.79, 28.51, 39.86, 40.38, 67.80, 79.50, 82.85, 101.39, 107.45, 109.62, 131.82, 161.44, 163.47, 168.48, 171.52, 176.74; HRMS  $m/z$  calcd for  $\text{C}_{20}\text{H}_{29}\text{N}_2\text{O}_6\text{S}$  425.1746 (M + H), found 425.1779.

**Stoichiometry of the Ligand–Fe(III) Complex.** The stoichiometry of each complex was determined spectrophotometrically for **10** at the  $\lambda_{\text{max}}$  (480 nm) of the visible absorption band of the ferric complex by the method given in detail in an earlier publication.<sup>93</sup> Briefly, a 0.5 mM iron(III) nitrilotriacetate (NTA) solution was made immediately before use by dilution of a 50 mM Fe(III)–NTA stock solution with TRIS buffer. Solutions of the ferric complex containing different ligand/Fe(III) ratios were then prepared by mixing appropriate volumes of 0.5 mM ligand in 100 mM TRIS Cl, pH 7.4, and 0.5 mM Fe(III)–NTA such that  $[\text{ligand}] + [\text{Fe}] = 1.00$  mM (constant). The Job's plot for the set of mixtures was then derived.

**Cell Culture.** Murine L1210 leukemia cells were maintained in logarithmic growth as a suspension culture in RPMI-1640 medium (Gibco, Grand Island, NY) containing 10% fetal bovine serum (Gibco), HEPES (14 mM)–MOPS (7 mM) buffer, 1 mM additional L-glutamine (Gibco), and 1 mM aminoguanidine at  $37^\circ\text{C}$  in a water-jacketed 5%  $\text{CO}_2$  incubator.

**IC<sub>50</sub> Determinations.** Cells were grown in 25-cm<sup>2</sup> tissue culture flasks in a total volume of 10 mL. Cultures were treated during logarithmic growth ( $0.5\text{--}1.0 \times 10^5$  cells/mL) with the compounds of interest as described previously.<sup>67</sup> Cell counting and calculation of percent of control growth were also carried out as given in an earlier publication.<sup>67</sup> The IC<sub>50</sub> is defined as the concentration of compound necessary to reduce cell growth to 50% of control growth after defined intervals of exposure.

**Uptake Determinations.** The molecules of interest were studied for their ability to compete with [<sup>3</sup>H]SPD for uptake into L1210 leukemia cell suspensions in vitro as given in detail in previous publications.<sup>61,65,67</sup> Briefly, cell suspensions were incubated in 1 mL of culture medium containing radiolabeled SPD alone or radiolabeled SPD in the presence of graduated

concentrations of chelator or derivative. At the end of the incubation period, the tubes were centrifuged; the pellet was washed, digested, and neutralized prior to scintillation counting. Lineweaver–Burk plots indicated simple competitive inhibition with respect to SPD.

**Compound Analysis.** During logarithmic growth, cells were treated with the compounds. At the end of the treatment period, cell suspensions were sampled, washed three times in ice-cold, incomplete medium, pelleted for extraction using 0.6 N perchloric acid,<sup>65</sup> and then freeze-fractured in liquid nitrogen/hot water three times. Each supernatant was frozen at  $-20^\circ\text{C}$  until analysis of analogue content by HPLC as described below.

**Cannulation of Bile Duct in Rats.** The cannulation has been described previously.<sup>88,94,95</sup> Briefly, male Sprague–Dawley rats averaging 450 g were housed in Nalgene plastic metabolic cages during the experimental period and given free access to water. The animals were anesthetized using sodium pentobarbital (55 mg/kg) administered intraperitoneally (ip). The bile duct was cannulated using 22-gauge polyethylene tubing. The cannula was inserted into the duct about 1 cm from the duodenum and tied snugly in place. After threading through the shoulder, the cannula was passed from the rat to the swivel inside a metal torque-transmitting tether, which was attached to a rodent jacket around the animal's chest. The cannula was directed from the rat to a Gilson microfraction collector (Middleton, WI) by a fluid swivel mounted above the metabolic cage. Bile samples were collected at 3-h intervals for up to 72 h. The urine samples were taken at 24-h intervals up to 72 h. Sample collection and handling were as previously described.<sup>88</sup>

**Drug Preparation and Administration for Rodent Studies.** Chelators **4**, **5**, **9**, and **10** were dissolved in water. The sodium salt of (S)-4'-(HO)-DADFT (**8**) was prepared by addition of the free acid to 1 equiv of NaOH. In the iron clearance assessments, all compounds were given sc to the rats at the doses shown in Table 2. For the metabolism experiments, conjugates **9** and **10** were administered sc at a dose of 300 mol/kg.

**Calculation of Iron Chelator Efficiency.** The theoretical outputs of the chelators were generated on the basis of a 3:1 ligand:iron complex for L1 (**4**) and its SPM conjugate (**5**) and on the basis of a 2:1 complex for desazadesferrithiocin analogue **8** and its NSPD conjugates **9** and **10**.<sup>93</sup> The efficiencies in the rodents were calculated as set forth previously.<sup>41,93,96</sup> Data are presented as the mean the standard error of the mean.

**Collection of Tissue Samples from Rodents.** Male Sprague–Dawley rats (250–350 g) were given the compounds prepared as described above sc. At times 2, 4, 6, 8, and 12 h after dosing with compound **9** ( $n = 4$  animals for the 2- and 4-h time points;  $n = 3$  for the 6-, 8-, and 12-h time points) or at times 2, 4, 6, 8, and 12 h after dosing with compound **10** ( $n = 5$  animals for the 2- and 4-h time points,  $n = 4$  for the 8-h time point, and  $n = 1$  for the 6- and 12-h time points), the liver was removed.

The liver samples were prepared for HPLC analysis by homogenizing in 0.6 N  $\text{HClO}_4$  at a ratio of 1:2 (w/v). The same volume of iron-free  $\text{H}_2\text{O}$  as  $\text{HClO}_4$  was then used to rinse the homogenizer probe; this rinse solution was added to the sample. This homogenate was centrifuged; the supernatant (200  $\mu\text{L}$ ) was injected onto the column.

**Analytical Methods. Terephthalic Acid–Polyamine Conjugates (6 and 7).** Analytical separation was performed on a Waters Symmetry C<sub>18</sub> column (250 mm  $\times$  4.6 mm, 5  $\mu\text{m}$ ) with guard column using a Rainin Instrument Co. HPLC system. The buffer employed was sodium octanesulfonate (2.5 mM) in potassium phosphate (25 mM), pH 3.0. Mobile phase A consisted of 5%  $\text{CH}_3\text{CN}$ , 95% buffer; mobile phase B consisted of 60%  $\text{CH}_3\text{CN}$ , 40% buffer. The solvent gradient program employed a linear gradient that increased from 20% mobile phase B to 40% mobile phase B over 40 min and a 5-min ramp to 100% B over 5 min. Postcolumn derivatization used a boric acid buffer system ( $\text{H}_3\text{BO}_3$ , 3.1% w/v; KOH, 2.6% w/v; 2-mercaptoethanol, 0.6% v/v) that contained *o*-phthalaldehyde (10 mL of a 4% w/v solution in  $\text{CH}_3\text{OH}$  per L of buffer).

The flow rate was 0.4 mL/min, isocratic; UV detection ( $\lambda_{\text{ex}}$ , 340 nm;  $\lambda_{\text{em}}$ , 445 nm) was utilized. This method had a detection limit of 0.07  $\mu\text{M}$ .

**Norspermidine-(S)-4'-(HO)-DADFT Conjugates (9 and 10).** Analytical separation was performed on a reversed-phase Supelco Discovery RP Amide C<sub>16</sub> column (150 × 4.6 mm, 5  $\mu\text{m}$ ) on the system described above, and UV detection was at 300 nm. The mobile phases were pumped at a flow rate of 1.5 mL/min. The buffer and mobile phases A and B were the same as described above. The solvent gradient program employed an initial 10-min isocratic portion with 5% mobile phase B (95% A), followed by a linear gradient increase to 80% mobile phase B at 35 min, a 5-min ramp to 100% B held for 10 min, and ramping back to 5% mobile phase B for 8 min (58–65 min total). This method had a detection limit of 0.2  $\mu\text{M}$  as a direct injection; this corresponds to a tissue concentration of 10 nmol/g of wet wt.

In both cases, the concentrations were calculated from the peak area fitted to calibration curves by nonweighted least squares linear regression with Rainin Dynamax HPLC Method Manager software (Rainin Instrument Co.).

#### Preparation of Sample and Method of Obtaining Mass Spectra of Diacid Metabolites of 10 after in Vivo Dosing.

A SupelClean C-18 cartridge of 1-mL capacity was used for solid-phase extraction (SPE) of the supernatant obtained after centrifugation of the liver homogenate from 2 h postdosing with 10. The packing in the cartridge was pretreated with CH<sub>3</sub>CN (2 mL) and washed with 3% (v/v) aqueous acetic acid solution (2 mL) before the application of the sample. After washing with 1% (v/v) aqueous acetic acid solution (2 mL), the sample was eluted with 300  $\mu\text{L}$  of a 74/25/1 (v/v) mixture of H<sub>2</sub>O, CH<sub>3</sub>CN, and glacial acetic acid for electrospray ionization (ESI) mass spectrometry.

ESI mass spectra were acquired on a quadrupole ion trap instrument (LCQ, ThermoFinnigan, San Jose, CA) operated with the manufacturer's Xcalibur 1.3 software. Mass spectra were acquired with an automatic gain control. Full-scan product ion spectra (MS/MS) were recorded at 1.0-u precursor ion isolation width, and the activation amplitude was adjusted to 1.75 V (35% of the maximum value) to obtain collision-induced dissociation (CID). Accurate mass measurements were performed on an Applied Biosystems (Foster City, CA) QSTAR XL hybrid quadrupole/time-of-flight instrument in the full-scan acquisition mode.

**Acknowledgment.** Funding was provided by the National Institutes of Health Grant No. R01-DK49108 and by Genzyme Drug Discovery and Development, Waltham, MA. NOESY was performed by James R. Rocca of the Advanced Magnetic Resonance Imaging and Spectroscopy Facility, University of Florida. We thank J. R. Timothy Vinson and Elizabeth M. Nelson for their development of the analytical methodology for the conjugates, Richard E. Smith and Samuel E. Algee for their aid in the preparation of the conjugates, and Dr. Eileen Eiler-McManis for her editorial and organizational assistance.

**Supporting Information Available:** Complete <sup>1</sup>H NMR spectra for reference compounds 27 and 28 employed in NOESY correlations and elemental analytical data for synthesized compounds. This material is available free of charge via the Internet at <http://pubs.acs.org>.

## References

- Olivieri, N. F.; Brittenham, G. M. Iron-chelating Therapy and the Treatment of Thalassemia. *Blood* **1997**, *89*, 739–761.
- Wonke, B. Clinical Management of  $\beta$ -Thalassemia Major. *Semin. Hematol.* **2001**, *38*, 350–359.
- Jellinger, K. A. The Role of Iron in Neurodegeneration. Prospects for Pharmacotherapy of Parkinson's Disease. *Drugs Aging* **1999**, *14*, 115–140.
- Hershko, C. Control of Disease by Selective Iron Depletion: A Novel Therapeutic Strategy Utilizing Iron Chelators. *Bailliere's Clin. Haematol.* **1994**, *7*, 965–1000.
- Bel, A.; Martinod, E.; Menasche, P. Cardioprotective Effect of Desferrioxamine. *Acta Haematol.* **1996**, *95*, 63–65.
- Raymond, K. N.; Carrano, C. J. Coordination Chemistry and Microbial Iron Transport. *Acc. Chem. Res.* **1979**, *12*, 183–190.
- Bergeron, R. J. Iron: A Controlling Nutrient in Proliferative Processes. *Trends Biochem. Sci.* **1986**, *11*, 133–136.
- Theil, E. C.; Huynh, B. H. Ferritin Mineralization: Ferroxidation and Beyond. *J. Inorg. Biochem.* **1997**, *67*, 30.
- Ponka, P.; Beaumont, C.; Richardson, D. R. Function and Regulation of Transferrin and Ferritin. *Semin. Hematol.* **1998**, *35*, 35–54.
- Babbs, C. F. Oxygen Radicals in Ulcerative Colitis. *Free Radic. Biol. Med.* **1992**, *13*, 169–181.
- Halliwell, B. Free Radicals and Antioxidants: A Personal View. *Nutr. Rev.* **1994**, *52*, 253–265.
- Hazen, S. L.; d'Avignon, A.; Anderson, M. M.; Hsu, F. F.; Heinecke, J. W. Human Neutrophils Employ the Myeloperoxidase-Hydrogen Peroxide-Chloride System to Oxidize  $\alpha$ -Amino Acids to a Family of Reactive Aldehydes. Mechanistic Studies Identifying Labile Intermediates along the Reaction Pathway. *J. Biol. Chem.* **1998**, *273*, 4997–5005.
- Finch, C. A.; Deubelbeiss, K.; Cook, J. D.; Eschbach, J. W.; Harker, L. A.; Funk, D. D.; Marsaglia, G.; Hillman, R. S.; Slichter, S.; Adamson, J. W.; Ganzoni, A.; Giblett, E. R. Ferrokinetics in Man. *Medicine (Baltimore)* **1970**, *49*, 17–53.
- Finch, C. A.; Huebers, H. A. Perspectives in Iron Metabolism. *N. Engl. J. Med.* **1982**, *306*, 1520–1528.
- Finch, C. A.; Huebers, H. A. Iron Metabolism. *Clin. Physiol. Biochem.* **1986**, *4*, 5–10.
- Hallberg, L. Bioavailability of Dietary Iron in Man. *Annu. Rev. Nutr.* **1981**, *1*, 123–147.
- Conrad, M. E.; Umbreit, J. N.; Moore, E. G. Iron Absorption and Transport. *Am. J. Med. Sci.* **1999**, *318*, 213–229.
- O'Connell, M. J.; Ward, R. J.; Baum, H.; Peters, T. J. The Role of Iron in Ferritin- and Haemosiderin-Mediated Lipid Peroxidation in Liposomes. *Biochem. J.* **1985**, *229*, 135–139.
- Seligman, P. A.; Klausner, R. D.; Huebers, H. A. Molecular Mechanisms of Iron Metabolism. In *The Molecular Basis of Blood Diseases*; Stamatoyannopoulos, G., Nienhuis, A. W., Leder, P., Majeris, P. W., Eds.; W. B. Saunders: Philadelphia, PA, 1987; p 219.
- Thomas, C. E.; Morehouse, L. A.; Aust, S. D. Ferritin and Superoxide-Dependent Lipid Peroxidation. *J. Biol. Chem.* **1985**, *260*, 3275–3280.
- Angelucci, E.; Brittenham, G. M.; McLaren, C. E.; Ripalti, M.; Baronciani, D.; Giardini, C.; Galimberti, M.; Polchi, P.; Lucarelli, G. Hepatic Iron Concentration and Total Body Iron Stores in Thalassemia Major. *N. Engl. J. Med.* **2000**, *343*, 327–331.
- Bonkovsky, H. L.; Lambrecht, R. W. Iron-Induced Liver Injury. *Clin. Liver Dis.* **2000**, *4*, 409–429, vi–vii.
- Pietrangelo, A. Mechanism of Iron Toxicity. *Adv. Exp. Med. Biol.* **2002**, *509*, 19–43.
- Cario, H.; Holl, R. W.; Debatin, K. M.; Kohne, E. Insulin Sensitivity and  $\beta$ -Cell Secretion in Thalassemia Major with Secondary Haemochromatosis: Assessment by Oral Glucose Tolerance Test. *Eur. J. Pediatr.* **2003**, *162*, 139–146.
- Wojcik, J. P.; Speechley, M. R.; Kertesz, A. E.; Chakrabarti, S.; Adams, P. C. Natural History of C282Y Homozygotes for Hemochromatosis. *Can. J. Gastroenterol.* **2002**, *16*, 297–302.
- Brittenham, G. M.; Griffith, P. M.; Nienhuis, A. W.; McLaren, C. E.; Young, N. S.; Tucker, E. E.; Allen, C. J.; Farrell, D. E.; Harris, J. W. Efficacy of Deferoxamine in Preventing Complications of Iron Overload in Patients with Thalassemia Major. *N. Engl. J. Med.* **1994**, *331*, 567–573.
- Brittenham, G. M. Disorders of Iron Metabolism: Iron Deficiency and Overload. In *Hematology: Basic Principles and Practice*, 3rd ed.; Hoffman, R., Benz, E. J., Shattil, S. J., Furie, B., Cohen, H. J., et al., Eds.; Churchill Livingstone: New York, 2000; pp 397–428.
- Zurlo, M. G.; De Stefano, P.; Borgna-Pignatti, C.; Di Palma, A.; Piga, A.; Melevendi, C.; Di Gregorio, F.; Burattini, M. G.; Terzoli, S. Survival and Causes of Death in Thalassemia Major. *Lancet* **1989**, *2*, 27–30.
- Bickel, H.; Hall, G. E.; Keller-Schierlein, W.; Prelog, V.; Vischer, E.; Wettstein, A. Metabolic Products of Actinomycetes. XXVII. Constitutional Formula of Ferrioxamine B. *Helv. Chim. Acta* **1960**, *43*, 2129–2138.
- Porter, J. B. Deferoxamine Pharmacokinetics. *Semin. Hematol.* **2001**, *38*, 63–68.
- Lee, P.; Mohammed, N.; Marshall, L.; Abeyasinghe, R. D.; Hider, R. C.; Porter, J. B.; Singh, S. Intravenous Infusion Pharmacokinetics of Desferrioxamine in Thalassemic Patients. *Drug Metab. Dispos.* **1993**, *21*, 640–644.
- Pippard, M. J.; Callender, S. T.; Finch, C. A. Ferrioxamine Excretion in Iron-Loaded Man. *Blood* **1982**, *60*, 288–294.

- (33) Pippard, M. J. Desferrioxamine-Induced Iron Excretion in Humans. *Bailliere's Clin. Haematol.* **1989**, *2*, 323–343.
- (34) Hoffbrand, A. V.; Al-Refaie, F.; Davis, B.; Siritanakatkul, N.; Jackson, B. F. A.; Cochrane, J.; Prescott, E.; Wonke, B. Long-term Trial of Deferiprone in 51 Transfusion-Dependent Iron Overloaded Patients. *Blood* **1998**, *91*, 295–300.
- (35) Olivieri, N. F. Long-term Therapy with Deferiprone. *Acta Haematol.* **1996**, *95*, 37–48.
- (36) Olivieri, N. F.; Brittenham, G. M.; McLaren, C. E.; Templeton, D. M.; Cameron, R. G.; McClelland, R. A.; Burt, A. D.; Fleming, K. A. Long-Term Safety and Effectiveness of Iron-Chelation Therapy with Deferiprone for Thalassemia Major. *N. Engl. J. Med.* **1998**, *339*, 417–423.
- (37) Richardson, D. R. The Controversial Role of Deferiprone in the Treatment of Thalassemia. *J. Lab. Clin. Med.* **2001**, *137*, 324–329.
- (38) Nisbet-Brown, E.; Olivieri, N. F.; Giardina, P. J.; Grady, R. W.; Neufeld, E. J.; Sechaud, R.; Krebs-Brown, A. J.; Anderson, J. R.; Alberti, D.; Sizer, K. C.; Nathan, D. G. Effectiveness and Safety of ICL670 in Iron-Loaded Patients with Thalassemia: a Randomised, Double-Blind, Placebo-Controlled, Dose-Escalation Trial. *Lancet* **2003**, *361*, 1597–1602.
- (39) Galanello, R.; Piga, A.; Alberti, D.; Rouan, M.-C.; Bigler, H.; Séchaud, R. Safety, Tolerability, and Pharmacokinetics of ICL670, a New Orally Active Iron-Chelating Agent in Patients with Transfusion-Dependent Iron Overload Due to  $\beta$ -Thalassemia. *J. Clin. Pharmacol.* **2003**, *43*, 565–572.
- (40) Nick, H.; Acklin, P.; Lattmann, R.; Buehlmayer, P.; Hauffe, S.; Schupp, J.; Alberti, D. Development of Tridentate Iron Chelators: From Desferrithiocin to ICL670. *Curr. Med. Chem.* **2003**, *10*, 1065–1076.
- (41) Bergeron, R. J.; Wiegand, J.; McManis, J. S.; McCosar, B. H.; Weimar, W. R.; Brittenham, G. M.; Smith, R. E. Effects of C-4 Stereochemistry and C-4' Hydroxylation on the Iron Clearing Efficiency and Toxicity of Desferrithiocin Analogues. *J. Med. Chem.* **1999**, *42*, 2432–2440.
- (42) Bergeron, R. J.; McManis, J. S.; Bussenius, J.; Brittenham, G. M.; Wiegand, J. Evaluation of the Desferrithiocin Pharmacophore as a Vector for Hydroxamates. *J. Med. Chem.* **1999**, *42*, 2881–2886.
- (43) Bergeron, R. J.; Wiegand, J.; McManis, J. S.; Weimar, W. R.; Huang, G. Structure–Activity Relationships Among Desazadesferrithiocin Analogues. *Adv. Exp. Med. Biol.* **2002**, *509*, 167–184.
- (44) Bergeron, R. J.; Wiegand, J.; McManis, J. S.; Bussenius, J.; Smith, R. E.; Weimar, W. R. Methoxylation of Desazadesferrithiocin Analogues: Enhanced Iron Clearing Efficiency. *J. Med. Chem.* **2003**, *46*, 1470–1477.
- (45) Bergeron, R. J.; Wiegand, J.; Weimar, W. R.; McManis, J. S.; Smith, R. E.; Abboud, K. A. Iron Chelation Promoted by Desazadesferrithiocin Analogues: An Enantioselective Barrier. *Chirality* **2003**, *15*, 593–599.
- (46) Bergeron, R. J.; Wiegand, J.; McManis, J. S.; Weimar, W. R.; Park, J.-H.; Eiler-McManis, E.; Bergeron, J.; Brittenham, G. M. Partition-Variant Desferrithiocin Analogues: Organ Targeting and Increased Iron Clearance. *J. Med. Chem.* **2005**, *48*, 821–831.
- (47) Bergeron, R. J.; Wiegand, J.; McManis, J. S.; Weimar, W. R.; Park, J.-H.; Eiler-McManis, E.; Bergeron, J.; Brittenham, G. M. Impact of the Lipophilicity of Desferrithiocin Analogues on Iron Clearance. In *Medicinal Inorganic Chemistry*; Sessler, J., Ed.; American Chemical Society: Washington, DC, 2005; in press.
- (48) Bergeron, R. J.; McManis, J. S.; Weimar, W. R.; Schreier, K. M.; Gao, F.; Wu, Q.; Ortiz-Ocasio, J.; Luchetta, G. R.; Porter, C.; Vinson, J. R. T. The Role of Charge in Polyamine Analogue Recognition. *J. Med. Chem.* **1995**, *38*, 2278–2285.
- (49) Bergeron, R. J.; Weimar, W. R.; Luchetta, G.; Streiff, R. R.; Wiegand, J.; Perrin, J.; Schreier, K. M.; Porter, C.; Yao, G. W.; Dimova, H. Metabolism and Pharmacokinetics of  $N^1,N^{11}$ -Diethylnorspermine. *Drug Metab. Dispos.* **1995**, *23*, 1117–1125.
- (50) Bergeron, R. J.; Weimar, W. R.; Luchetta, G.; Sninsky, C. A.; Wiegand, J. Metabolism and Pharmacokinetics of  $N^1,N^{14}$ -Diethylhomospermine. *Drug Metab. Dispos.* **1996**, *24*, 334–343.
- (51) Bergeron, R. J.; Merriman, R. L.; Olson, S. G.; Wiegand, J.; Bender, J.; Streiff, R. R.; Weimar, W. R. Metabolism and Pharmacokinetics of  $N^1,N^{11}$ -Diethylnorspermine in a *Cebus apella* Primate Model. *Cancer Res.* **2000**, *60*, 4433–4439.
- (52) Bergeron, R. J.; Wiegand, J.; Weimar, W. R.; Lindstrom, T. C.; Fannin, T. L.; Ratliff-Thompson, K. A Comparison of Iron Chelator Efficacy in Iron Overloaded Beagle Dogs and Monkeys (*Cebus apella*). *Comp. Med.* **2004**, *54*, 641–649.
- (53) Cohen, S. S. *A Guide to the Polyamines*; Oxford University Press: New York, 1998; p 624.
- (54) Porter, C. W.; Kramer, D. L.; Bernacki, R. J.; Bergeron, R. J. Regulation of Polyamine Biosynthetic Activity and Homeostasis as a Novel Antiproliferative Strategy. *Dev. Oncol.* **1992**, *68*, 325–344.
- (55) Seiler, N.; Dezeure, F. Polyamine Transport in Mammalian Cells. *Int. J. Biochem.* **1990**, *22*, 211–218.
- (56) Seiler, N.; Delcros, J. G.; Moulinoux, J. P. Polyamine Transport in Mammalian Cells. An Update. *Int. J. Biochem. Cell Biol.* **1996**, *28*, 843–861.
- (57) Porter, C. W.; McManis, J.; Casero, R. A.; Bergeron, R. J. Relative Abilities of Bis(ethyl) Derivatives of Putrescine, Spermidine, and Spermine to Regulate Polyamine Biosynthesis and Inhibit L1210 Leukemia Cell Growth. *Cancer Res.* **1987**, *47*, 2821–2825.
- (58) Bergeron, R. J.; Neims, A. H.; McManis, J. S.; Hawthorne, T. R.; Vinson, J. R. T.; Bortell, R.; Ingeno, M. J. Synthetic Polyamine Analogues as Antineoplastics. *J. Med. Chem.* **1988**, *31*, 1183–1190.
- (59) Pegg, A. E.; Madhubala, R.; Kameji, T.; Bergeron, R. J. Control of Ornithine Decarboxylase Activity in  $\alpha$ -Difluoromethylornithine-resistant L1210 Cells by Polyamines and Synthetic Analogues. *J. Biol. Chem.* **1988**, *263*, 11008–11014.
- (60) Porter, C. W.; Bergeron, R. J. Enzyme Regulation as an Approach to Interference with Polyamine Biosynthesis—an Alternative to Enzyme Inhibition. *Adv. Enzyme Regul.* **1988**, *27*, 57–79.
- (61) Bergeron, R. J.; Hawthorne, T. R.; Vinson, J. R. T.; Beck, D. E., Jr.; Ingeno, M. J. Role of the Methylene Backbone in the Antiproliferative Activity of Polyamine Analogues on L1210 Cells. *Cancer Res.* **1989**, *49*, 2959–2964.
- (62) Libby, P. R.; Bergeron, R. J.; Porter, C. W. Structure–Function Correlations of Polyamine Analog-Induced Increases in Spermidine/Spermine Acetyltransferase Activity. *Biochem. Pharmacol.* **1989**, *38*, 1435–1442.
- (63) Porter, C. W.; Pegg, A. E.; Ganis, B.; Madhubala, R.; Bergeron, R. J. Combined Regulation of Ornithine and *S*-Adenosylmethionine Decarboxylases by Spermine and the Spermine Analogue  $N^1,N^{12}$ -Bis(ethyl)spermine. *Biochem. J.* **1990**, *268*, 207–212.
- (64) Bernacki, R. J.; Bergeron, R. J.; Porter, C. W. Antitumor Activity of  $N,N'$ -Bis(ethyl)spermine Homologues against Human MALME-3 Melanoma Xenografts. *Cancer Res.* **1992**, *52*, 2424–2430.
- (65) Bergeron, R. J.; McManis, J. S.; Liu, C. Z.; Feng, Y.; Weimar, W. R.; Luchetta, G. R.; Wu, Q.; Ortiz-Ocasio, J.; Vinson, J. R. T.; Kramer, D.; Porter, C. Antiproliferative Properties of Polyamine Analogues: A Structure–Activity Study. *J. Med. Chem.* **1994**, *37*, 3464–3476.
- (66) Bergeron, R. J.; Feng, Y.; Weimar, W. R.; McManis, J. S.; Dimova, H.; Porter, C.; Raisler, B.; Phanstiel, O. A Comparison of Structure–Activity Relationships between Spermidine and Spermine Analogue Antineoplastics. *J. Med. Chem.* **1997**, *40*, 1475–1494.
- (67) Bergeron, R. J.; Müller, R.; Bussenius, J.; McManis, J. S.; Merriman, R. L.; Smith, R. E.; Yao, H.; Weimar, W. R. Synthesis and Evaluation of Hydroxylated Polyamine Analogues as Antiproliferatives. *J. Med. Chem.* **2000**, *43*, 224–235.
- (68) Bergeron, R. J.; Müller, R.; Huang, G.; McManis, J. S.; Algee, S. E.; Yao, H.; Weimar, W. R.; Wiegand, J. Synthesis and Evaluation of Hydroxylated Polyamine Analogues as Antiproliferatives. *J. Med. Chem.* **2001**, *44*, 2451–2459.
- (69) Bergeron, R. J.; Weimar, W. R.; Wu, Q.; Feng, Y.; McManis, J. S. Polyamine Analogue Regulation of NMDA MK-801 Binding: A Structure–Activity Study. *J. Med. Chem.* **1996**, *39*, 5257–5266.
- (70) Delcros, J.-G.; Tomasi, S.; Carrington, S.; Martin, B.; Renault, J.; Blagbrough, I. S.; Uriac, P. Effect of Spermine Conjugation on the Cytotoxicity and Cellular Transport of Acridine. *J. Med. Chem.* **2002**, *45*, 5098–5111.
- (71) Bergeron, R. J.; Yao, G. W.; Yao, H.; Weimar, W. R.; Sninsky, C. A.; Raisler, B.; Feng, Y.; Wu, Q.; Gao, F. Metabolically Programmed Polyamine Analogue Antidiarrheals. *J. Med. Chem.* **1996**, *39*, 2461–2471.
- (72) Bergeron, R. J.; McManis, J. S.; Franklin, A. M.; Yao, H.; Weimar, W. R. Polyamine-Iron Chelator Conjugate. *J. Med. Chem.* **2003**, *46*, 5478–5483.
- (73) Geall, A. J.; Blagbrough, I. S. Homologation of Polyamines in the Rapid Synthesis of Lipospermine Conjugates and Related Lipoplexes. *Tetrahedron* **2000**, *56*, 2449–2460.
- (74) Israel, M.; Rosenfield, J. S.; Modest, E. J. Analogues of Spermine and Spermidine. I. Synthesis of Polymethylenepolyamines by Reduction of Cyanoethylated  $\alpha,\omega$ -Alkylenediamines. *J. Med. Chem.* **1964**, *7*, 710–716.
- (75) Sasaki, H.; Suehiro, A.; Nakamoto, Y. Cyclophanes. VIII. Synthesis and DNA-Cleaving Activities of Novel Heterocyclophanes Containing Two 4,4'-Bithiazole Rings. *Chem. Pharm. Bull. (Tokyo)* **1997**, *45*, 189–193.

- (76) Bergeron, R. J.; Garlich, J. R. Amines and Polyamines from Nitriles. *Synthesis* **1984**, 782–784.
- (77) Nagarajan, M.; Xiao, X.; Antony, S.; Kohlhagen, G.; Pommier, Y.; Cushman, M. Design, Synthesis, and Biological Evaluation of Indenoisoquinoline Topoisomerase I Inhibitors Featuring Polyamine Side Chains on the Lactam Nitrogen. *J. Med. Chem.* **2003**, *46*, 5712–5724.
- (78) Nakamura, Y. Actinocinyl-Bis(hemin); DNA-Intercalating Cleavage Agent. *Heterocycles* **1988**, *27*, 1873–1879.
- (79) Corey, E. J.; Dittami, J. P. Total Synthesis of ( $\pm$ )-Ovalicin. *J. Am. Chem. Soc.* **1985**, *107*, 256–257.
- (80) Quintana, R. P.; Lasso, A.; Queen, G. S.; Baldwin, C. M. Aspirin Analogues with Enhanced Interfacial Activity. *J. Colloid Interface Sci.* **1981**, *83*, 146–152.
- (81) Robertson, D. W.; Beedle, E. E.; Krushinski, J. H.; Pollock, G. D.; Wilson, H.; Wyss, V. L.; Hayes, J. S. Structure–Activity Relationships of Arylimidazopyridine Cardiotonics: Discovery and Inotropic Activity of 2-[2-Methoxy-4-(methylsulfinyl)phenyl]-1*H*-imidazo[4,5-*c*]pyridine. *J. Med. Chem.* **1985**, *28*, 717–727.
- (82) van Deun, R.; Binnemans, K. Influence of the Ligand Structure on the Liquid Crystalline Properties of Lanthanide-Containing Salicylaldehyde Mesogens. *Liquid Crystals* **2003**, *30*, 479–486.
- (83) Nudelman, A.; Bechor, Y.; Falb, E.; Fischer, B.; Wexler, B. A.; Nudelman, A. Acetyl Chloride as a Convenient Reagent for: A) Quantitative Formation of Amine Hydrochlorides B) Carboxylate Ester Formation C) Mild Removal of N-t-BOC-Protective Group. *Synth. Commun.* **1998**, *28*, 471–474.
- (84) Lebreton, L.; Annat, J.; Derrepas, P.; Dutartre, P.; Renaut, P. Structure-Immunosuppressive Activity Relationships of New Analogues of 15-Deoxyspergualin. 1. Structural Modifications of the Hydroxyglycine Moiety. *J. Med. Chem.* **1999**, *42*, 277–290.
- (85) Hu, W.; Reder, E.; Hesse, M. 177. Electrospray-Ionization Mass Spectrometry. Part 2. Neighboring-Group Participation in the Mass-Spectral Decomposition of 4-Hydroxycinnamoyl-spermidines. *Helv. Chim. Acta* **1996**, *79*, 2137–2151.
- (86) Selig, R. A.; White, L.; Gramacho, C.; Sterling-Levis, K.; Fraser, I. W.; Naidoo, D. Failure of Iron Chelators to Reduce Tumor Growth in Human Neuroblastoma Xenografts. *Cancer Res.* **1998**, *58*, 473–478.
- (87) Bergeron, R. J.; Streiff, R. R.; Wiegand, J.; Vinson, J. R. T.; Luchetta, G.; Evans, K. M.; Peter, H.; Jenny, H.-B. A Comparative Evaluation of Iron Clearance Models. *Ann. N. Y. Acad. Sci.* **1990**, *612*, 378–393.
- (88) Bergeron, R. J.; Wiegand, J.; Dionis, J. B.; Egli-Karmakka, M.; Frei, J.; Huxley-Tencer, A.; Peter, H. H. Evaluation of Desferri-thiocin and Its Synthetic Analogues as Orally Effective Iron Chelators. *J. Med. Chem.* **1991**, *34*, 2072–2078.
- (89) Bergeron, R. J.; Streiff, R. R.; Wiegand, J.; Luchetta, G.; Creary, E. A.; Peter, H. H. A Comparison of the Iron-Clearing Properties of 1,2-Dimethyl-3-hydroxypyrid-4-one, 1,2-Diethyl-3-hydroxypyrid-4-one, and Deferoxamine. *Blood* **1992**, *79*, 1882–1890.
- (90) Seiler, N. Polyamine Oxidase, Properties and Functions. *Prog. Brain Res.* **1995**, *106*, 333–344.
- (91) Seiler, N. Oxidation of Polyamines and Brain Injury. *Neurochem. Res.* **2000**, *25*, 471–490.
- (92) Bergeron, R. J.; Wiegand, J.; McManis, J. S.; Weimar, W. R.; Smith, R. E.; Algee, S. E.; Fannin, T. L.; Slusher, M. A.; Snyder, P. S. Polyamine Analogue Antidiarrheals: A Structure–Activity Study. *J. Med. Chem.* **2001**, *44*, 232–244.
- (93) Bergeron, R. J.; Wiegand, J.; Weimar, W. R.; Vinson, J. R. T.; Bussenius, J.; Yao, G. W.; McManis, J. S. Desazadesmethyl-desferri-thiocin Analogues as Orally Effective Iron Chelators. *J. Med. Chem.* **1999**, *42*, 95–108.
- (94) Bergeron, R. J.; Wiegand, J.; Brittenham, G. M. HBED: A Potential Alternative to Deferoxamine for Iron-Chelating Therapy. *Blood* **1998**, *91*, 1446–1452.
- (95) Bergeron, R. J.; Wiegand, J.; Wollenweber, M.; McManis, J. S.; Algee, S. E.; Ratliff-Thompson, K. Synthesis and Biological Evaluation of Naphthyl-desferri-thiocin Iron Chelators. *J. Med. Chem.* **1996**, *39*, 1575–1581.
- (96) Bergeron, R. J.; Wiegand, J.; Brittenham, G. M. HBED: The Continuing Development of a Potential Alternative to Deferoxamine for Iron-Chelating Therapy. *Blood* **1999**, *93*, 370–375.
- (97) Although four animals were originally employed for the 8-h time point, the levels of the free acid **10**, but not any of the metabolites, in both the liver and the pancreas were 9-fold higher in one animal than in the other three animals. Accordingly, this animal was not included in the calculations used to derive the 8-h time point shown in Figure 8B.

JM048974F